2020-05

Process Simulation of Methanol Production from Water Electrolysis and Tri-Reform

Shi, Chenxu

UNIVERSITY OF CALGARY

Process Simulation of Methanol Production from Water Electrolysis and Tri-Reforming

by

Chenxu Shi

A THESIS
SUBMITTED TO THE FACULTY OF GRADUATE STUDIES
IN PARTIAL FULFILMENT OF THE REQUIREMENTS FOR THE
DEGREE OF MASTER OF SCIENCE

GRADUATE PROGRAM IN CHEMICAL ENGINEERING

CALGARY, ALBERTA

MAY, 2020

Abstract

The alarmingly increase in anthropogenic CO_2 emissions is widely considered as the root cause of global warming. To mitigate this issue, CO_2 utilization via methanol production can be an effective approach. The present study develops an innovative process to produce methanol by combining water electrolysis with tri-reforming of methane (TRM). The proposed process utilizes carbon-free electricity to split water into O_2 and H_2; O_2 is collected for partial oxidation reaction in the TRM and H_2 is collected for stoichiometric number (SN) optimization. This process configuration eliminates the typical problem of H_2 deficiencies associated with methanol synthesis and allows for additional CO_2 to be converted. The main process flowsheet is developed with the well-known Aspen HYSYS process simulator. Then the feasibility of this project is evaluated based on its techno-economic performance as well as greenhouse gas (GHG) emissions. The estimated capital expenditure (CAPEX), operating expenditure (OPEX) and GHG emissions of the baseline plant are $774 million, $263 million/year and -0.14 $kgCO_2eq/kgMeOH$, respectively. In particular, water electrolysis process accounts for 34% of CAPEX and 54% of OPEX. A discounted cash flow (DCF) model combined with sensitivity analyses show that a breakeven point can be reached with a methanol price of $491/ton. The results from this study demonstrate that combining water electrolysis with TRM can improve the sustainability and economic viability for methanol production. However, in order for the process to become more financially attractive, further research and development are necessary to drive down the costs of the current water electrolysis technology.

Acknowledgements

I would like to express my most sincere gratitude to my supervisor Dr. Nader Mahinpey for his continuous support and encouragements throughout my journey as an MSc student. It has truly been a great learning experience to work under his supervision.

I would like to thank my supervisory committee members and examiners, Dr. Roman Shor and Dr. Hua Song, for taking their valuable time to review my thesis and offering their constructive feedbacks.

I would like to acknowledge Babak Labbaf for his continuous support on my research project. His presence motivated me to push for progress everyday on my thesis.

I would like to thank the past and present members of the Energy and Environment Research Group (EERG). I consider myself lucky to be surrounded by the most supportive, engaging and knowledgeable peers. This journey certainly would not have been the same without them.

I would also like to express my sincere appreciation to all the sponsors of our EERG group including Natural Sciences and Engineering Research Council of Canada (NSERC), Canadian Natural Resources Limited (CNRL) and Devon Energy Corporation, for their kind financial support.

In addition, I would like to extend my gratitude to all the rest of the staff members in the Chemical and Petroleum Engineering Department at the University of Calgary. Their

day-to-day work behind the scenes created an efficient and welcoming environment for all students.

Last, but most importantly, I would like to thank my parents, Wenqi Shi and Lihua Chen. Without their constant love and support, I would not have been able to come this far.

Dedication

I dedicate this work to the scientific community.

Table of Contents

List of Tables

List of Figures

Nomenclature

AC	alternating current
AR5	Fifth Assessment Report
ASU	air separation unit
ATR	auto-thermal reforming
AWE	alkaline water electrolysis
BWR	boiling water reactor
C&SU	commissioning and start-up
CAPEX	capital expenditure
CEPCI	Chemical Engineering Plant Cost Index
CLC	chemical looping combustion
DC	direct current
DCF	discounted cash flow
GHG	greenhouse gas
GHSV	Gas hourly space velocity
GHV	gross heating value
GWP_{100}	100-year global warming potential
HHV	higher heating value
HPS	high pressure steam
IGCC	integrated gasification combined cycle
IPCC	Intergovernmental Panel on Climate Change
IRR	internal rate of return
LHHW	Langmuir-Hinshelwood-Hougen-Watson
NPT	net payout time
NPV	net present value
NRTL	non-random two-liquid
OPEX	operating expenditure

PEM	proton exchange membrane
PFR	plug flow reactor
POX	partial oxidation
SN	stoichiometric number
SRM	steam reforming of methane
tkUCE	ThyssenKrupp Uhde Chlorine Engineers
TRM	tri-reforming of methane
WGS	water gas shift
WHB	waste heat boiler

Chapter One: **Introduction**

1.1 Background

Methanol is one of the most useful chemical compounds in modern society. By developing relevant chemistry, methanol can be used for a great variety of purposes from making synthetic petrochemical products to energy related applications. Within the petrochemical industry, methanol is frequently used as a precursor for a wide range of synthetic materials and chemicals. Some common products derived from methanol include adhesives, foams, solvents and windshield washer fluids [1]. More recently, there has also been a growing demand for methanol in the energy sector. In comparison to most energy carriers, methanol is a relatively cleaner fuel. The molecular structure of methanol consists of a methyl group attached to a hydroxyl group with no carbon-carbon bonds. Therefore, this allows methanol to generate much less air pollutants during combustion [2]. Today, approximately 45% of the produced methanol worldwide is used for energy related applications and this number is projected to grow in the upcoming years [1].

One of the renowned interests of using methanol is motivated by Professor George A Olah with his original concept, the "Methanol Economy" [3]. This concept is aimed to gradually phase out fossil fuel consumption by switching to methanol as the default energy carrier. On a human time-scale, fossil fuel is considered a non-renewable resource [4]. The massive consumption of fossil fuel also generates a significant amount of air pollutions including greenhouse gas (GHG) emissions. Therefore, for the long term sustainability of global energy supply and prevention of climate change, it was identified that methanol can be considered a suitable alternative. The volumetric energy density of

methanol is higher in comparison to hydrogen [5]. Methanol also has a relatively high boiling point (64.7°C) and low freezing point (-97.6°C), which makes it relatively safe for pipeline transportation and storage [6]. In the event of an accidental spill, methanol would have less environmental impact compared to crude oil or gasoline since it can be reduced through natural processes such as photo-oxidation and biodegradation [7]. Finally, the process of methanol production often involves CO_2 as a precursor, which is a promising solution to counter global GHG emissions.

In order to fully achieve the "Methanol Economy", it is important to understand how methanol is produced. The history of methanol production started with Robert Boyle when he first isolated pure methanol using the process of wood distillation [8]. This process was capable of producing relatively small volumes and is initially used for lighting, cooking and heating purposes. However, as the demand for methanol grows for industrial applications, a more economical approach was desired. In 1905, Paul Sabatier and Jean-Baptiste Senderens discovered that copper can effectively catalyze the decomposition of methanol. It was hypothesized that the same material under alternative conditions can be equally effective for the production of methanol [9]. This work was later expanded through patents to become the first synthetic pathway for large-scale methanol production.

Since then, the methanol industry has evolved to become more diverse and efficient. A variety of raw materials and pathways for methanol production are employed and many more are under development for future applications [7], [8]. Figure 1.1 shows a generic block flow diagram of the current process for methanol production. This process involves

the three basic steps of syngas generation, methanol synthesis and product purification. The available feedstock used for the syngas generation process can include anything from fossil fuels such as natural gas, crude oil and coal to renewable fuels such as biomass, landfill and plant emissions [10]. The decision for choosing the appropriate feedstock was vastly based on economic considerations. Since the early days, natural gas has been the predominant feedstock for methanol production as they are relatively abundant and inexpensive. With the recent commercialization of hydraulic fracturing, the price of natural gas was further reduced [11]. As a result, currently about 90% of the world's methanol are derived from natural gas [12]. The cost advantage of natural gas does not necessarily apply to all geographical locations. In areas where natural gas is scarce or unavailable, the cost of shipping and transportation may render the process too expensive for implementation. Under such scenarios, other types of feedstock may become the preferred choice for methanol production. An example of this is in China where coal became the predominant feedstock for methanol production [9], [13].

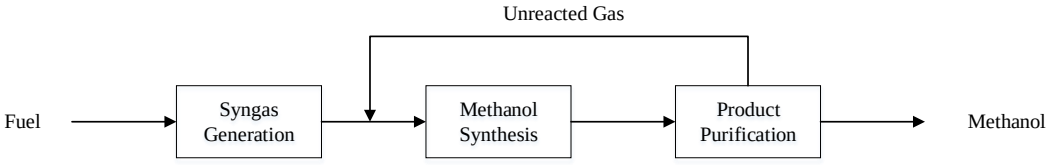

Figure 1. 1 Basic block flow diagram of the conventional methanol synthesis process

As discussed, fossil fuels are considered non-renewable resources. Yet, it is still heavily relied upon by the current methanol industry. In addition, the processes of converting fossil fuels into methanol also typically generate a considerable amount of CO_2 emissions. In order to achieve greater sustainability, there is now a growing interest in

alternative processes through green chemistry. An example of this can be found in Iceland, where Carbon Recycling International (CRI) has constructed the world's first commercial methanol plant using only CO_2 and hydrogen. The process implemented by CRI is commonly referred to as the direct CO_2 hydrogenation. The CO_2 comes from an adjacent geothermal power station where it is also supplying energy to make hydrogen. This plant began operations early in 2012 and is currently able to produce 4000 tons of methanol and recycle 5500 tons of CO_2 annually [14]. One of the drawbacks of this process is that it is limited by the costs of H_2 manufacturing [8]. Although it can be justified in Iceland due to its readily available geothermal energy, but for most other places in the world, the process of making hydrogen through water electrolysis can be highly expensive. Furthermore, many literature studies have suggested that direct CO_2 hydrogenation would be less competitive overall in comparison to traditional syngas process. The reason may be due to additional water formation on the commercial Cu/ZnO catalyst which leads to inactivity and ultimately reduces the methanol yield [15], [16].

1.2 Objective

The main objective of this thesis is to develop a novel process for methanol production that overcomes the challenges of direct CO_2 hydrogenation. By using a combination of tri-reforming of methane and water electrolysis, high quality syngas can be generated while utilizing CO_2 as a feedstock. This proposed design is set to achieve net negative carbon emissions and reach far superior economic performance than direct CO_2 hydrogenation.

1.3 Thesis Structure

This thesis contains elements of both manuscript-based and traditional thesis, all in accordance with the University of Calgary FGS guidelines. The main body of this thesis consists of three chapters (Chapters 2, 3 and 4). Chapter 2 is a literature review on the current research progress and technologies available for syngas generation and methanol synthesis. Chapter 3 highlights the design and conceptualization of a novel methanol plant through process modeling. This chapter contains all the key elements on simulation setup, flow sheet developments as well as results and outcomes. Based on the process simulation, Chapter 4 is a recently published technical and economic analysis paper that focuses on CO_2 utilization and methanol production. This work was primarily carried out by Chenxu Shi under the supervision of Dr. Nader Mahinpey and with the help and support from Babak Labbaf and Ehsan Mostafavi.

Chapter Two: **Literature Review**

2.1 Chapter Overview

The goal of this chapter is to gather the relevant information in support of the thesis objective. Since methanol production is a highly integrated process with multiple unit operations, this literature review is only focused on the most relevant topics which are syngas generation and methanol synthesis. The first section of this chapter looks at a variety of syngas generation processes including steam reforming, dry reforming, partial oxidation, auto-thermal reforming, and tri-reforming. These processes are examined based on their principal operations as well as advantages and disadvantages. The second section is focused on methanol synthesis, which can be further divided into topics focused on reaction mechanisms and kinetics as well as reactor design configurations. All of the information obtained from this chapter is used to guide decisions in choosing the appropriate technologies and parameters for process modeling.

2.1 Syngas Generation

Syngas is a mixture of H_2, CO, and CO_2. The specific molar ratio of syngas can vary significantly based on the feedstock and manufacturing process. The method of syngas characterization is mostly based on the stoichiometric number (SN), which is a molar ratio between the difference of H_2 and CO_2 and the summation of CO and CO_2 [8]:

$$\mathrm{SN} = \frac{\text{moles } \mathrm{H_2} - \text{moles } \mathrm{CO_2}}{\text{moles } \mathrm{CO} + \text{moles } \mathrm{CO_2}} \tag{2.1}$$

Ideally for methanol synthesis, SN should be equal to 2 or slightly higher [8], [17]. This is due to the reaction stoichiometry of methanol synthesis. If the SN value is greater than 2, excess hydrogen would be accumulated downstream in the methanol synthesis loop. On the other hand, if the SN value is less than 2, this would result in hydrogen deficit. Both cases are less than optimal for the overall productivity of methanol. In practice, it is often difficult to achieve a SN value of 2 due to limitations of the existing technologies. This point will be further elaborated in the following sections.

2.2.1 Steam Reforming of Methane

Steam reforming of methane (SRM) is the most widely adopted technology for syngas generation. In this process, steam is co-fed together with natural gas to a reformer furnace typically operated in the range of 800 – 1000°C and 20 – 30 atm. [18]. The main reactions are [19]:

$$CH_4 + H_2O \leftrightarrow CO + 3H_2, \quad \Delta H^o = 206 \text{ kJ mol}^{-1} \tag{2.2}$$

$$CO + H_2O \leftrightarrow CO_2 + H_2, \quad \Delta H^o = -41 \text{ kJ mol}^{-1} \tag{2.3}$$

Since the overall reaction is highly endothermic, an external heat supply must be available in order to drive the reaction forward. This is often achieved by burning a portion of the natural gas feed, but this leads to substantial production and emission of CO_2 in the flue gas stream. Furthermore, the typical SRM process produces syngas at a SN of approximately 3 [8], [20]. As a result, excess H_2 is generated downstream in the methanol synthesis loop and would have to be either purged or used as a plant fuel gas. Nevertheless, SRM currently remains as the preferred choice for methanol production due to its economic viability and level of technological maturity.

2.2.2 Dry Reforming of Methane

Dry reforming of methane (DRM) or also known as CO_2 reforming of methane is a syngas generation process that has received much attention in literatures. The main benefit of this process is that CO_2 can be utilized as a feedstock, which has the potential to reduce the impact of GHG emissions. The main reactions for DRM are [21]:

$$CH_4 + CO_2 \leftrightarrow 2CO + 2H_2, \quad \Delta H^o = 247 \text{ kJ mol}^{-1} \tag{2.4}$$

$$CO + H_2O \leftrightarrow CO_2 + H_2, \quad \Delta H^o = -41 \text{ kJ mol}^{-1} \tag{2.5}$$

In many design aspects, DRM is similar to SRM. The overall reaction is also highly endothermic which necessitates an external heat supply. Water gas shift is also present in this process as a common side reaction. However, contrary to SRM, this process is more susceptible to catalyst deactivation due to increased coke formation. Since CO_2 is introduced as a feed, the reduction of CO_2 can result in additional coke formation [22]. Another drawback of this process is that the produced syngas has a low SN of 1. For methanol synthesis, this would lead to H_2 deficiency during operations and would necessitate an additional source of H_2 to balance the reaction stoichiometry and increase productivity.

2.2.3 Partial Oxidation of Methane

Partial oxidation of methane (POX) is another potentially attractive option for syngas generation. POX is a combustion process with limited amount of oxygen. As a result, this creates incomplete combustion and produces carbon monoxide and hydrogen [23]. The main reaction set for POX is [8]:

$$CH_4 + \tfrac{1}{2} O_2 \leftrightarrow CO + 2H_2, \quad \Delta H^o = -35.6 \text{ kJ mol}^{-1} \tag{2.6}$$

$$CO + ½\ O_2 \leftrightarrow CO_2, \quad \Delta H^o = -283\ kJ\ mol^{-1} \tag{2.7}$$

$$H_2 + ½\ O_2 \leftrightarrow H_2O, \quad \Delta H^o = -241\ kJ\ mol^{-1} \tag{2.8}$$

The overall reaction is exothermic and the process can be either thermal (TPOX) or catalytic (CPOX) [24]. No indirect heat supply is required. POX can be an attractive option because it requires less energy and capital investment in comparison to SRM [25]. The produced syngas has a theoretical SN of 2, but the actual achievable SN is less than 2 because of unwanted oxidation reactions (2.7 and 2.8) that forms additional CO_2 and H_2O [8], [26]. Nevertheless, the SN from POX is comparatively more suitable for methanol production than either SRM or DRM. Despite the advantages, POX is not commonly used by the methanol industry due to several drawbacks. First, POX generally requires pure oxygen and the need for an air separation plant may offset the potential economic advantage it brings. If air is used instead of oxygen, then nitrogen would have to be separated downstream which can end up being more costly. Second, due to POX's exothermic nature, a lot of excess heat is produced and wasted which would result in lower energy efficiency. Lastly, due to the typical high operating temperatures of POX, process safety and reliability can be another major concern [23].

2.2.4 Auto Thermal Reforming

Auto thermal reforming (ATR) is a heat neutral process for syngas production[8], [26]. This process has gained much popularity in the current methanol industry because it eliminates the need of external heat supply. The reaction stoichiometry of this process is the combination between SRM and POX reactions. The ATR reactor is generally divided into 3 reaction zones as shown in Figure 2.2 [27]:

1. Burner – where the inlet gases are mixed together in a turbulent flame

2. Combustion zone – where the exothermic POX reaction takes place
3. Catalytic zone – where the endothermic SRM reaction takes place

The heat generated from the exothermic POX reactions are direct consumed in the catalytic SRM reactions. The overall reaction can be expressed in the following manner [28]:

$$CH_4 + (2 - 2x)\, H_2O + x\,(O_2) \leftrightarrow CO_2 + (4 - 2x)\, H_2, \quad \Delta H^{o} = -35.6 \text{ kJ mol}^{-1} \qquad (2.9)$$

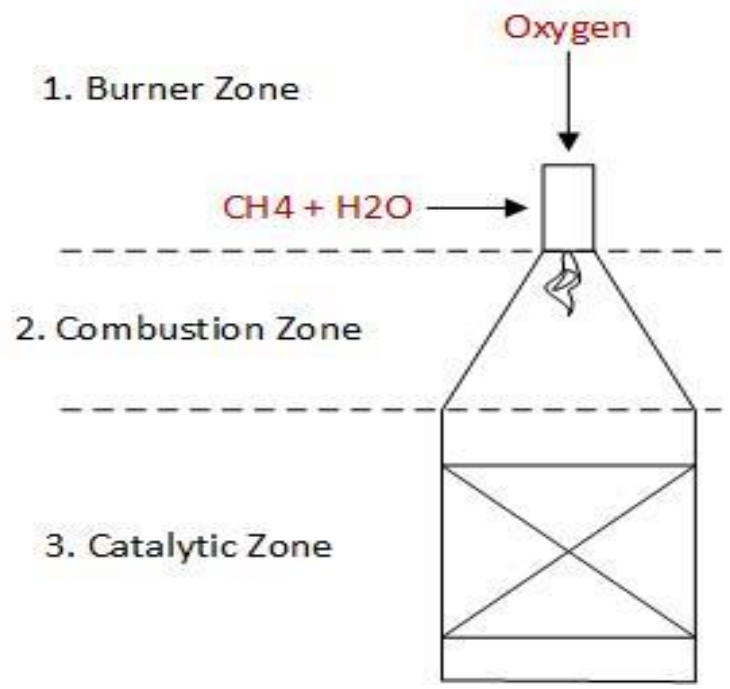

Figure 2. 2 ATR reactor configuration

An advantage of ATR is that no flue gas is generated, which means the overall process generates significantly less GHG emissions than the traditional SRM. Furthermore, because the heat produced from the POX reaction in the combustion chamber is immediately consumed for the steam reforming reactions, this allows the process to be more energy efficient than standalone POX. Another major advantage of the ATR

process is that the SN can be adjusted by changing the oxygen-to-carbon (O/C) and steam-to-carbon (S/C) ratios [29]. This allows the ATR to be flexible at producing syngas for different types of applications including methanol synthesis. The disadvantage of ATR is similar to POX in that it requires an air separation unit (ASU) and this will require additional capital investment.

2.2.5 Tri-reforming of Methane

Tri-reforming of methane (TRM) can be seen as a variation of ATR. The main difference is that CO_2 is also introduced to the feed together with steam, oxygen and natural gas. This reaction stoichiometry of TRM can be viewed as a combination between SRM, DRM and POX put together. The SN can be adjusted by altering the feed ratios between oxygen, steam, CO_2 and natural gas. Since CO_2 is also being introduced in the feed, the resulting SN would be generally less than 2 [30]. Therefore, unless there is an additional source of hydrogen, using this process for methanol synthesis would be less suitable than the standard ATR.

2.3 Methanol Synthesis

The current methanol synthesis reaction is typically carried out in gas phase and using copper based catalyst. The reaction conditions are generally between 200 – 300°C and 50 – 100 bar. In the whole methanol industry, about 60% uses the Johnson Matthey process and another 27% uses the Lurgi process [8]. Process design variations are mostly associated with catalyst arrangements and reactor configurations [31].

2.3.1 Kinetics and Modeling

Kinetics is one of the most important aspects of chemical reactor design. Understanding the reaction kinetic mechanisms can help determine the optimal operating conditions and

catalyst arrangements. This study focuses on the commercial Cu/ZnO catalyst, which is most widely used in the methanol industry. Currently in literatures, the reaction mechanism involved in methanol synthesis is still an open issue for debate. It is generally accepted that methanol is predominately formed by the hydrogenation of CO_2. However, the macro kinetics for methanol synthesis can be described by three overall reactions [32]:

$$CO_2 + 3H_2 \rightarrow CH_3OH + H_2O, \quad \Delta H^o = -49 \text{ kJ mol}^{-1} \tag{2.10}$$

$$CO + 2H_2 \rightarrow CH_3OH, \quad \Delta H^o = -49 \text{ kJ mol}^{-1} \tag{2.11}$$

$$CO + H_2O \leftrightarrow CO_2 + H_2, \quad \Delta H^o = -41 \text{ kJ mol}^{-1} \tag{2.12}$$

A large number of kinetic equations have been proposed in literature. Different studies have looked at various feed gas compositions and operating conditions. Amongst the literature sources, Vanden Bussche and Froment's rate equation is one of the most widely used models for methanol simulation studies. Based on this reaction scheme, H_2 and CO_2 are adsorbed onto the copper active sites forming carbonate structures [32]. Subsequently, these carbonate structures are converted through series of hydrogenation reactions before forming methanol. Between 15 to 51 bar and 180 to 280°C, this model is able to adequately describe the effect of pressure, temperature and feed composition on product composition.

2.3.1 Reactors

Since methanol synthesis via CO and CO_2 hydrogenation is a highly exothermic process, therefore, temperature control is a necessary consideration in order to maximize yield. Currently, the methanol industry has adopted two common types of reactors, adiabatic and isothermal [8]. The most common type of adiabatic reactor used in industry is the

low pressure quench converter developed by Johnson Matthey. This type of reactor consists of multiple adiabatic beds installed in series. The beds are loaded with catalyst, generally consisting of $Cu/ZnO/Al_2O_3$. In between each bed, either water or gas can be injected to cool the reactants. This reactor configuration can handle a maximum capacity of 3000 t/d [8].

The Lurgi converter or commonly referred to as the boiling water reactor (BWR) is the most widely adopted reactor in the entire methanol industry. The design is a fixed bed reactor similar to that of a shell-and-tube heat exchanger. The catalyst is loaded inside the reactor tubes and cooling water is injected on the shell side. This type of configuration allows for tight control on the reactor temperature profile and is able to generate high pressure steam (HPS) at the same time.

Chapter Three: **Process Modeling**

3.1 Chapter Overview

This chapter is focused on the conceptualization of a methanol plant that combines the technologies of tri-reforming of methane and water electrolysis. The simulation work is carried out using Aspen HYSYS v10 simulator with 15 components and 3 different fluid packages. Process information on the feed streams is shown in Table 3.1. Majority of the process is modelled using the Peng-Robinson fluid package. For the purification system in particular, the liquid phase separation between methanol and water is modelled using the Non-random two-liquid (NRTL) fluid package. Lastly, the steam generation and cooling water systems is modelled using the ASME steam fluid package. The simulation converged with a mass balance error of 0.00% and an energy balance error of 0.04%. The main simulation flowsheet is shown in Figure 3.1. Note that Figure 3.1 also contains 6 individual sub-flowsheets, each with a designed purpose.

Table 3. 1 Process information for the feed streams

Feed	Natural gas [33]	CO_2 [34]	Demineralized water
Feed rate (t/h)	36.1	29.8	45.0
Vapor Fraction	1	1	0
Temperature (ºC)	40	300	25
Pressure (kPaa)	2749	2549	2500
Composition (mol%)	C_1: 93.90 C_2: 4.20 C_3: 0.30 C_{4+}: 0.10 N_2: 1.0 O_2: 0.01 H_2O: 0.0 CO_2: 0.50	CO_2: 99.5 H_2O: 0.5	H_2O: 100.0

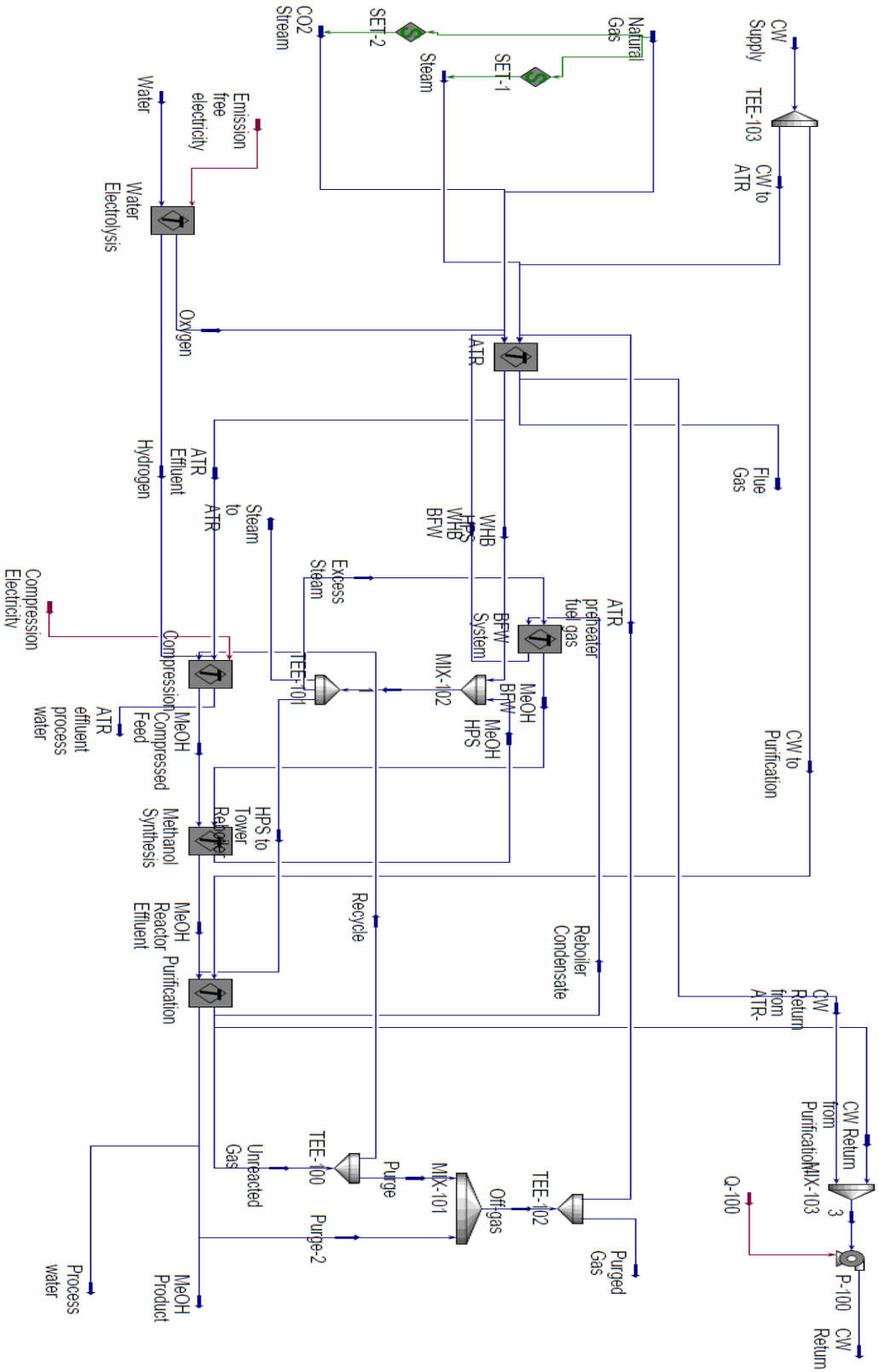

Figure 3. 1 Main simulation flowsheet

3.2 Tri-reforming System

Figure 3.2 shows the tri-reforming system modeled in Aspen HYSYS. Pipeline natural gas, steam, post combustion captured CO_2 and oxygen are fed together to the process to produce syngas. The major unit operations are fired heater, pre-reformer, tri-reformer and waste heat boiler. Since pipeline natural gas has already been pre-treated with sulfur removal, it is not necessary to be considered again in this simulation. The fired heater is modeled using a Gibbs reactor. It is supplied with purged gas from the methanol synthesis loop and combustion air. There is no required make-up fuel gas in this process. The fired heater acts as a multi-pass preheater for the reactants that provides a total heat duty of 42 MW. Due to the absence of reliable kinetic data for reforming reactions in literature, both the pre-reformer and the ATR are also modeled using the Gibbs reactor. The pre-reforming reaction is an endothermic process and it is operated at a temperature of 550°C. This process eliminates the C2+ hydrocarbons in the feed before it is sent to the ATR. The ATR is an energy neutral process. The partial oxidation reaction provides the heat required for SRM and DRM. The effluent from the ATR consists of mostly syngas and is at a high temperature of 1046°C. A waste heat boiler is used to cool the effluent down to 265°C while generating high pressure steam.

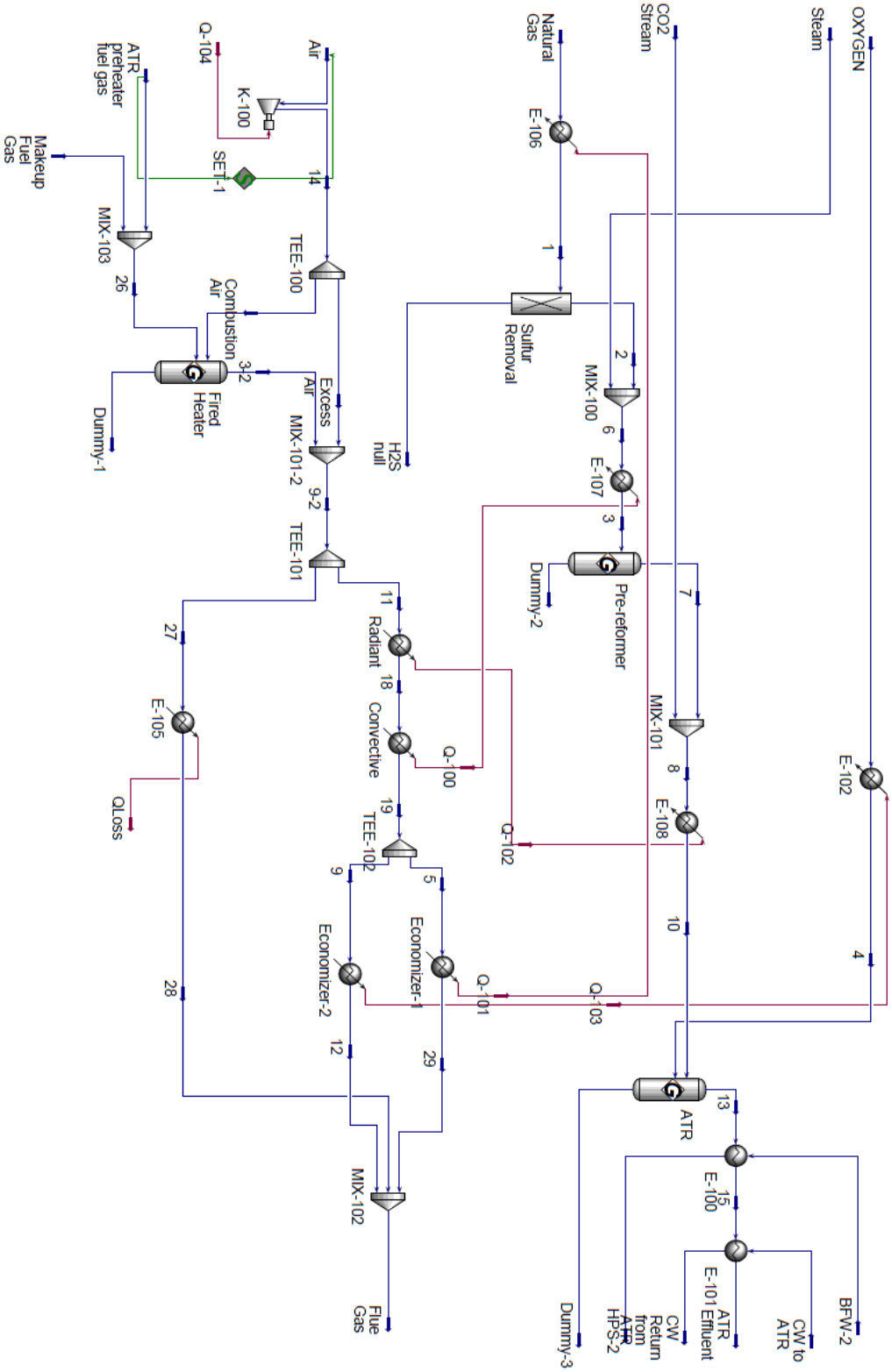

Figure 3. 2 Simulation sub-flowsheet: Tri-Reforming System

3.3 Water Electrolysis System

Figure 3.3 shows the water electrolysis system modeled in Aspen HYSYS. Since HYSYS has limited capabilities with modeling electrolytes, only a simplified model was built to represent the actual process. The major unit operations are a conversion reactor followed by a component splitter. Demineralized water is fed to the conversion reactor with a specified 100% conversion to form H_2 and O_2. Since the reaction is highly endothermic, energy is supplied in the form of electricity to the reactor. It is worth mentioning that the efficiency cannot be explicitly specified in this reactor, which means that in order to account for the total energy consumption of this process, it is necessary to carry out manual energy calculations. Using the efficiency factor provided in literature [35], it was determined that the total energy consumption for this process is 300 MW. The component splitter separates the produced gases into separate streams of H_2 and O_2 at 99.95% purity.

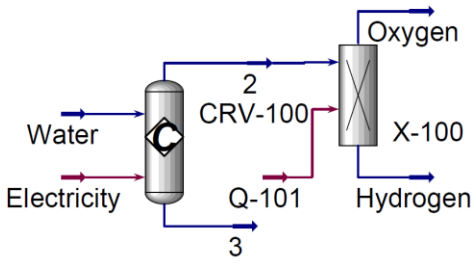

Figure 3. 3 Simulation sub-flowsheet: Water Electrolysis System

3.4 Compression System

Figure 3.4 shows the compression system modeled in Aspen HYSYS. ATR effluent is dehydrated before it is mixed with hydrogen from water electrolysis. After the mix, the syngas feed has a SN of 2.0 and is ready to be send for compression. The main unit operations of the compression system are the two-staged centrifugal compressor for the

syngas feed and a single-staged centrifugal compressor for the recycled gas. The syngas compressor is set to a pressure ratio of 2.2 per stage and a polytrophic efficiency of 80%. The recycled gas compressor is set to match the outlet pressure from the syngas compressor. Based on this configuration, the final outlet pressure is at 10670 kPa and the recycling ratio is 4.67.

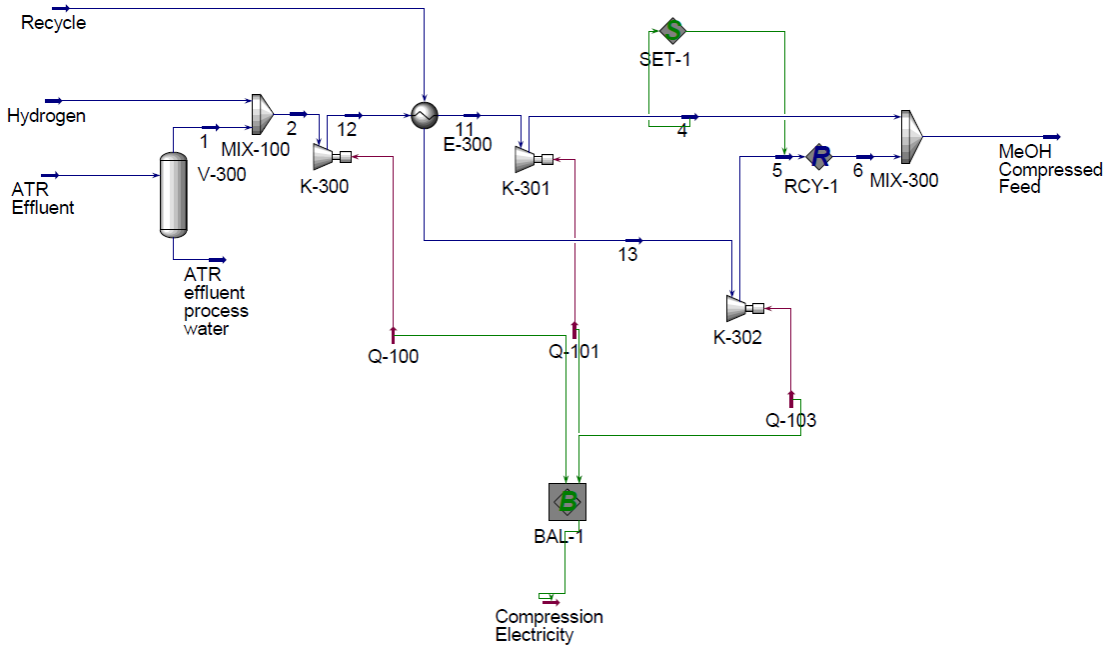

Figure 3. 4 Simulation sub-flowsheet: Compression System

3.5 Methanol Synthesis System

Figure 3.4 shows the methanol synthesis system modeled in Aspen HYSYS. The two main unit operations are the feed/effluent exchanger (E-400) and the boiling water reactor (BWR). E-400 is a standard shell and tube heat exchanger that heats up the syngas to 250°C while cooling down the BWR effluent. The BWR is modeled using a plug flow reactor with a heterogeneous catalyst reaction set. The selected catalyst for this model is

$Cu/ZnO/Al_2O_3$ with the well-known kinetics expression developed by Bussche and Froment [32]. However, due to the specific input template on HYSYS, the kinetic expressions had to be re-arranged in order to be modeled correctly. Please see Appendix A for more details on the kinetics expression re-arrangement steps. The overall reactor design of the BWR is similar to a shell-and-tube exchanger. The methanol synthesis reaction occurs on the tube side and saturated water passes on the shell side to keep the temperature profile under control. There are a total of 2700 tubes, each with a length of 7.0 m and a diameter of 0.035 m. This makes up the total volume of the reactor to be 18.2 m^3 with a void fraction of 0.4. The single pass conversion for H_2, CO, and CO_2 are 15.7%, 27.3%, and 9.0%, respectively. The BWR effluent exits at a temperature of 275°C.

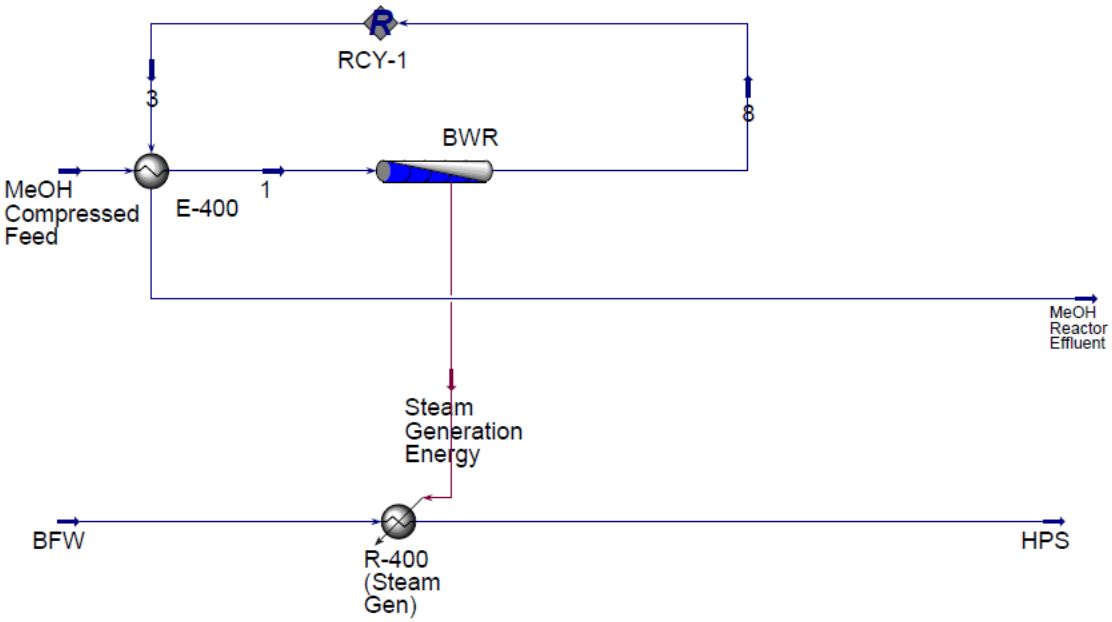

Figure 3. 5 Simulation sub-flowsheet: Methanol Synthesis

3.6 Purification System

Figure 3.6 shows the purification system modeled in Aspen HYSYS. The main unit operations are the two separators (V-501 and V-502) and the distillation column (T-100). V-501 is the main separator of the unreacted gases from the BWR effluent. It is operated at 40°C and 10200 kPa. 96% of methanol and 98% of water is condensed and separated from the unreacted gases. V-502 is a secondary separator operated at 40°C and at a reduced pressure of 250 kPa. With this condition, most of the unreacted gases are vaporized and separated from the methanol/water mixture. The last step of purification is at T-100 where the methanol is separated from water. T-100 is contains 22 equilibrium stages, a partial condenser and a partial reboiler. The feed is introduced at stage 12, methanol is collected at the top and water is collected at the bottom. The final recovery rate of methanol is at 99.5% with 99.9wt% purity.

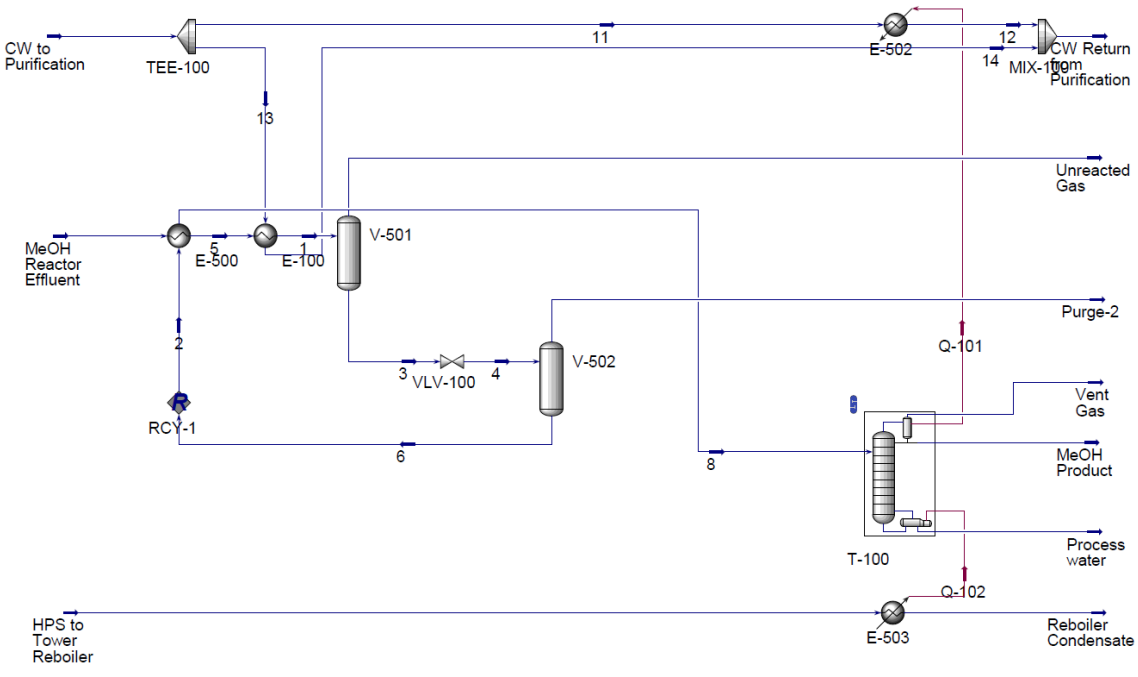

Figure 3. 6 Simulation sub-flowsheet: Purification System

3.7 Boiler Feed Water System

Figure 3.7 shows the boiler feed water return system. Boiler feed water in this process is sent to the WHB in the tri-reforming system and the BWR in the methanol synthesis system. The water gets converted to steam and is mostly used for the distillation column reboiler. Another small portion of the steam is used for syngas generation. There is an excess amount of steam which can be used for auxiliary heating purposes. Once the steam is used for heating, the returned condensate is pumped back to the BFW surge drum and ready to be re-used. A make-up water stream is necessary since the BFW system is not entirely kept in a closed loop, part of the steam is consumed for syngas generation.

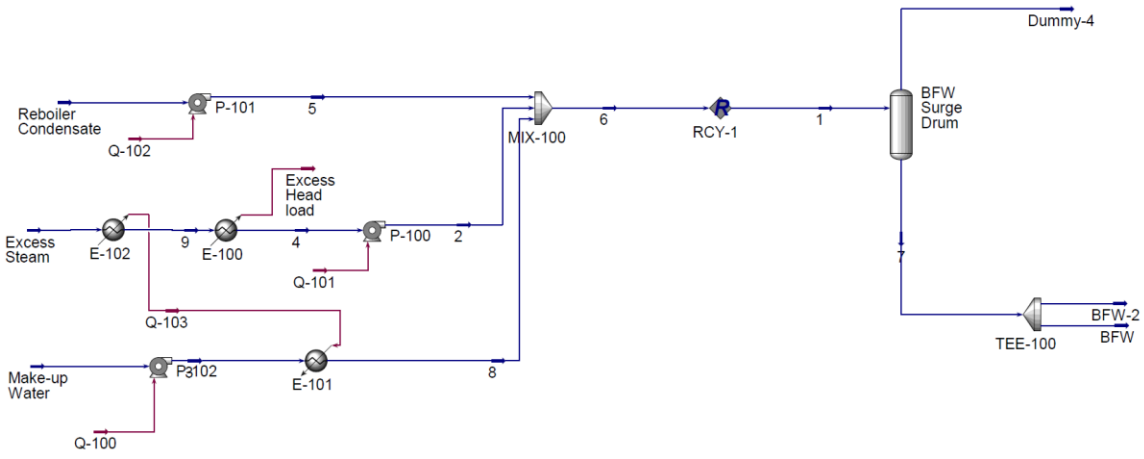

Figure 3. 7 Simulation sub-flowsheet: Boiler Feed Water System

Chapter Four: **Methanol Production from Water Electrolysis and Tri-Reforming: Process Design and Technical-Economic Analysis**

Accepted on Dec. 27, 2019 in the *Journal of CO_2 Utilization*

4.1 Chapter Overview

This chapter is a manuscript titled "Methanol Production from Water Electrolysis: Process Design and Technical-Economic Analysis", which was recently published in the Journal of CO_2 Utilization. No changes were made on the original contents aside from page formatting and word editing. For more information on the estimation of CAPEX and OPEX from this study, please refer to Appendix B and Appendix C. This study was carried out at the EERG group supervised by Dr. Nader Mahinpey. He also provided support on methodology development and technical reviews. Babak labbaf and Ehsan Mostafavi provided useful feedbacks and suggestions on the process simulation. Chenxu Shi was responsible for overall project conceptualization and implementation. This manuscript proposed a novel concept for methanol production and completed with environmental and economic feasibility studies.

4.2 Abstract

CO_2 utilization via methanol synthesis can be an effective approach to mitigate the issue of global warming. This study developed an innovative process to produce methanol by combining water electrolysis with tri-reforming of methane (TRM). The proposed design utilized carbon-free electricity to split water into O_2 and H_2; O_2 is collected for partial oxidation reaction in the TRM and H_2 is collected for stoichiometric number (SN) optimization. This process configuration eliminates the typical problems of H_2 surplus or deficit associated with methanol synthesis and allows a substantial amount of CO_2 to be converted. The main process flowsheet was developed with Aspen HYSYS process

simulator and then the feasibility of this project was evaluated based on its technical, environmental, and economic performances. The estimated capital expenditure (CAPEX), operating expenditure (OPEX) and GHG emissions of the baseline plant are US$774 million, US$263 million/yr. and -0.14 $kgCO_2eq/kgMeOH$, respectively. In particular, water electrolysis process accounted for 34% of CAPEX and 51% of OPEX. A discounted cash flow (DCF) model combined with sensitivity analyses showed that a breakeven point could be reached with a methanol price of US$491/ton. The results demonstrated that combining water electrolysis with TRM could achieve a sustainable carbon-sink process for methanol production.

4.3 Introduction

The methanol economy proposed by Nobel Prize winner, Professor George A. Olah is a concept that aims to ensure the long-term stability of global energy supply and the environment [7]. Through the development of relevant chemistry, methanol can be adapted as a transportation fuel, an energy storage medium, and as a raw material for various petrochemical products [3]. Methanol is a relatively clean fuel in comparison to most other energy carriers. The molecular structure of methanol consists of mostly hydrogen atoms and no carbon-carbon bonds [36]. This allows methanol to generate significantly less air pollutants such as NO_x, SO_2 and particulate matters during combustion. In the case of an accidental spill into the environment, methanol would have lower impact compared to the counterpart of crude oil or gasoline. This is because methanol can degrade more rapidly through the processes of photo-oxidation and biodegradation [8]. Owing to its wide range of industrial applications and environmental benefits, it is of great interest for society to adopt methanol as the main energy carrier.

Today, about 90% of the world's methanol comes from natural gas [12], a non-renewable energy resource. For the long-term sustainability of the methanol industry and the world at large, it is imperative to come up with feasible process designs that utilize renewable energy. Methanol synthesis through green chemistry is a widely studied topic in literatures. One of the commonly suggested pathways is the direct hydrogenation of CO_2 to methanol, where the CO_2 comes from a carbon capture process and the H_2 comes from water electrolysis using renewable electricity (wind, solar, geothermal, biomass, etc.). Van-Dal and Bouallou studied such a process configuration through the development of an Aspen Plus simulation model [37]. Their work concluded that as long as the H_2 produced is carbon-free, the methanol plant itself is able to mitigate large amounts of CO_2 emissions. In support of this finding, other feasibility studies have also led to similar conclusions that CO_2 hydrogenation can be a promising approach to counter global emissions [38], [39]. In fact, the concept of direct CO_2 hydrogenation is not new to industry as well. Some of the earliest methanol plants in the US used byproducts of fermentation, which consisted of CO_2 and H_2, for methanol production [40]. In 2011, Carbon Recycling International (CRI) of Iceland commercialized the world's first CO_2-to-methanol plant using its readily available geothermal energy [41]. The same company has already announced plans to construct additional pilot plants throughout Europe [42], [43]. In Japan, CO_2-to-methanol process was also demonstrated by Mitsui Chemicals using a pilot plant in order to assess its feasibility [44].

Despite having all the environmental benefits, direct CO_2 hydrogenation to methanol has its own challenges to overcome. Through a comprehensive review study by Bozzano and Manenti, it was suggested that methanol synthesis based on water electrolysis is not an

attractive option due to its high energy consumptions associated with H_2 manufacturing [8]. Likewise, Perez-Fortes et al. have also identified that the current H_2 production costs would be too high for this process to be financially attractive [39]. The economic viability of this process is based on the premises that electricity is available at extremely low cost, which, for the short to medium term, is an unrealistic condition to achieve in most geographic locations. In addition to the high costs associated with H_2 production, several studies have also pointed out other technical challenges associated with direct CO_2 hydrogenation. Pontzen et al. performed a study on the commercial Cu/ZnO catalyst (Süd-Chemie) and reported that CO_2 hydrogenation is slower and less competitive compare to CO hydrogenation under typical process conditions [15]. Tijm et al. also identified that higher CO_2 concentration creates irreversible damages to the commercial Cu/ZnO catalyst and the root cause of the problem is may be due to water formation during the synthesis reaction [16]. Therefore, in order to prolong the lifespan of the catalysts, the presence of CO plays an important role by actively consuming water via water gas shift (WGS) to form additional CO_2 and H_2. This is also reflected during industrial operations when Haldor Topsoe reported that a higher ratio of CO to CO_2 can increase reaction rate and conversion per pass and decrease catalyst deactivation rate [17].

In order to overcome the challenges of direct CO_2 hydrogenation, one of the new areas being studied is oxidative methane reforming process coupled with water electrolysis. Combining these two processes enables the generation of high quality syngas that is optimal for methanol synthesis. Since water electrolysis generates oxygen as a byproduct, it can be directly used in the natural gas reforming process through partial oxidation.

With this configuration, the costly air separation unit (ASU) can be eliminated. Furthermore, since there is additional H_2 available from water electrolysis, this allows more CO_2 to be utilized in the reforming process in order to balance the syngas composition. Li et al. proposed this configuration through their study of plasma catalytic reforming coupled with water electrolysis [45]. Despite being mostly focused on the lab-scale performance of the plasma catalytic reformer (PCR), their work demonstrated that high energy efficiencies can be achieved with this configuration. In this current project, we are focused on combining the state-of-the-art technologies of tri-reforming of methane and alkaline water electrolysis for methanol synthesis. The combined technologies are investigated through process development and technical-economic analysis. It is predicted that such a configuration can achieve significantly better economic performance than direct CO_2 hydrogenation. The main portion of this work is performed utilizing Aspen HYSYS process simulator and the results from the simulation are used to conduct further assessments on the technical, economic and environmental performance. Specifically, the technical metrics are focused on overall CO_2 conversion and net energy efficiency, the economical metrics are focused on the capital expenditure (CAPEX), operating expenditure (OPEX) and net present value (NPV), and the environmental metrics are geared towards greenhouse gas (GHG) emissions. The results obtained are placed in parallel comparison with published data of direct CO_2 hydrogenation in order to identify areas of strengths and weaknesses.

4.4 Technology Overview

When considering the design criteria for methanol synthesis, one of the key aspects to consider is the composition of syngas. This is often characterized by the stoichiometric

number (SN), which is a molar ratio of the difference between H_2 and CO_2 to the summation of CO and CO_2:

$$\mathrm{SN} = \frac{\text{moles } \mathrm{H_2} - \text{moles } \mathrm{CO_2}}{\text{moles CO} + \text{moles } \mathrm{CO_2}} \tag{4.2}$$

For methanol production under ideal conditions, SN should be equal to a value of 2 or slightly higher [8], [17]. Any significant deviation from a SN of 2 would lead to cases of hydrogen surplus (SN >2) or hydrogen deficiency (SN<2). In the traditional steam reforming of methane (SMR) process, the generated syngas typically has a SN of 2.8 to 3 [8]. As a result, this creates excess H_2, which is then usually recycled to the reformer as fuel gas. Another emerging trend in the methanol industry is to consider the possibility of a stand-alone auto-thermal reforming (ATR) for syngas generation. However, since this arrangement produces syngas at a lower SN of 1.7, it was suggested that an additional source of H_2 to balance the stoichiometry would make the process more effective [9]. Hence, the general approach considered in this study is the combination of water electrolysis with tri-reforming (TRM) to produce syngas followed by conversion to methanol. The process utilizes carbon-free electricity to split water into O_2 and H_2; O_2 is collected for the partial oxidation reaction in tri-reforming and H_2 is collected for the optimization of SN for methanol production. Figure 4.1 shows the block flow diagram of the conceptual design. Within the battery limit of the central processing facility contains five main subsystems: water electrolysis, tri-reforming, syngas compression, methanol synthesis reaction, and methanol purification. Technology selections of each subsystem are discussed in details in the sections below.

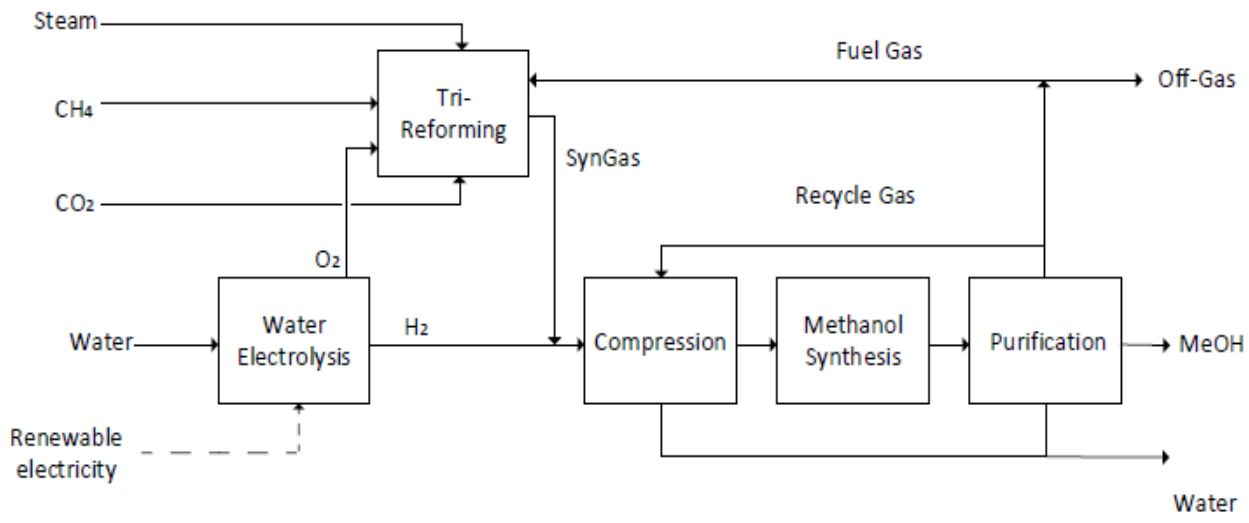

Figure 4. 1 Block flow diagram of the methanol synthesis process

4.4.1 Water electrolysis system

Water electrolysis using carbon-free electricity is a sustainable way to produce H_2 and O_2. The two most common types of commercially available technologies are alkaline water electrolysis (AWE) and proton exchange membrane (PEM). AWE is a more established technology in comparison to PEM. Despite having relatively lower power density than PEM, AWE offers longer stability, lower cost and higher power capacity [46]. From a technical and economic standpoint, this study selected AWE to be the more appropriate technology for the generation of H_2 and O_2.

A typical AWE system consists of anode and cathode, electrolyte, diaphragm and power supply. In general, caustic electrolytes such as potassium hydroxide solution are used to avoid corrosion problems. The electrodes are typically made of nickel due to its operational reliability and low cost [47]–[49]. The purpose of the diaphragm is to separate the produced H_2 and O_2; this prevents the formation of an explosive gas mixture

and maintain high product purities. When a sufficient direct current (DC) is applied, the following reactions occur simultaneously on both the cathode and anode,

Cathode: $2H^+ + 2e \rightarrow H_2$ (4.2)

Anode: $2OH^- \rightarrow 1/2O_2 + H_2O + 2e$ (4.3)

The overall reaction of the water electrolysis process is:

$$H_2O \rightarrow H_2 + 1/2\ O_2 \quad (4.4)$$

This study considers the nominal 20-MW AWE module developed by ThyssenKrupp Uhde Chlorine Engineers (tkUCE). Each module produces 4000 Nm3/h of H_2. The tkUCE AWE cells also have a wide operating range of 10% to 100%, which makes it suitable for the intermittent nature of wind and solar electricity. The designed operating pressure is slightly above atmospheric pressure and the cells are able to generate products at >99.95% purity [35]. The complete installation package also includes an AC/DC converter, gas compressors and temporary storage vessels for H_2 and O_2.

4.4.2 Tri-reforming system

Syngas can be generated from a variety of different processes. However, considering the objectives of this study, tri-reforming of methane (TRM) was selected as the suitable technology. The TRM process is designed to convert natural gas together with steam, CO_2 and O_2. Instead of using an air separation unit (ASU), this process can take full advantage of the available O_2 generated from water electrolysis. Furthermore, the produced syngas ratio can be adjusted by altering the amount of steam and CO_2 fed to the system [50], [51]. In comparison to dry reforming which also converts CO_2, coke formation is significantly suppressed due to the presence of steam [26], [52].

The main reactor of TRM takes the identical form of an auto-thermal reformer (ATR) with three reaction zones [27]: the burner where the inlet feed mixes in a turbulent diffusion flame, the combustion zone where partial oxidation reaction (POX) occurs and the catalytic zone where steam and dry reforming reactions (SRM and DRM) occur. For the purpose of this study, a commercial Ni/Al_2O_3 catalyst is used in the main reactor and the reactions considered herein are,

POX: $CH_4 + 1/2O_2 \rightarrow CO + 2H_2, \quad \Delta H^o = -35.6 \text{ kJ mol}^{-1}$ (4.5)

SRM: $CH_4 + H_2O \leftrightarrow CO + 3H_2, \quad \Delta H^o = 206.8 \text{ kJ mol}^{-1}$ (4.6)

DRM: $CH_4 + CO_2 \leftrightarrow 2CO + 2H_2, \quad \Delta H^o = 247.3 \text{ kJ mol}^{-1}$ (4.7)

To maximize the operating life expectancy of such a reactor, inlet natural gas must go through feed pre-treatment. This process typically consists of desulfurization and pre-reforming reactions. During desulfurization, H_2 is reacted with sulfur compounds contained in the feed to form H_2S and is separated it from the main process. This prevents catalyst poisoning in the main reactor and allows for longer operations without catalyst replacement. In the pre-reforming process, C_{2+} hydrocarbons are eliminated through reactions with steam thereby preventing soot formation and deposition in the main reactor. Like the main TRM reactor, the same Ni/Al_2O_3 catalyst is also used in the pre-reformer.

4.4.3 Compression system

The compression system follows a standardized industry approach. In order to handle a large quantity of syngas, the most common design is to use multi-staged centrifugal compressor with inter-stage cooling. To prevent liquid entrainment and damage to the compressor bearings, a liquid knockout drum with demister pad is installed.

4.4.4 Methanol synthesis system

The methanol synthesis process converts syngas into methanol. The reaction kinetics considered in this study is based on the commercial Cu/ZnO catalyst commonly used in industry. Through wide consensus in literatures, methanol is predominately formed by the hydrogenation of CO_2 [8]. Any presence of CO must first undergoes water gas shift (WGS) to form CO_2 and H_2 before it can be converted to methanol [26]. For this reason, the Langmuir-Hinshelwood-Hougen-Watson (LHHW) kinetic expression developed by Bussche and Froment [32] is adopted for reactor modeling. These kinetic expressions are shown in Table 4.1. The overall kinetic reactions considered in this study are,

CO_2 hydrogenation: $CO_2 + 3H_2 \rightarrow CH_3OH + H_2O, \quad \Delta H^o = -49 \text{ kJ mol}^{-1}$ (4.8)

WGS: $CO + H_2O \leftrightarrow CO_2 + H_2, \quad \Delta H^o = -41 \text{ kJ mol}^{-1}$ (4.9)

The study selected the widely used boiling water reactor (BWR) for methanol synthesis. Since the overall reaction is highly exothermic, heat energy must be removed to maximize product yield. The BWR is similar in design to that of a shell-and-tube heat exchanger by which methanol synthesis reaction occurs on the tube side and water vaporizes on the shell side. The tubes are filled with $Cu/ZnO/Al_2O_3$ commercial catalyst pellets to speed up the reaction and the water from the shell side absorbs the heat released. Such a reactor design keeps the temperature under control and generates high-pressure steam (HPS) at the same time.

Table 4. 1 Kinetic expressions for $Cu/ZnO/Al_2O_3$ catalyst

<table>
<tr><td colspan="2">Methanol Synthesis:

$r_{CH3OH} = \frac{k_1 P_{CO2} P_{H2}\left(1-\frac{1}{K_{eq1}}\frac{P_{H2O}P_{CH3OH}}{P_{H2}^3 P_{CO2}}\right)}{\left(1+k_2\frac{P_{H2O}}{P_{H2}}+k_3 P_{H2}^{0.5}+k_4 P_{H2O}\right)^3}$</td><td colspan="2">WGS:

$r_{WGS} = \frac{k_5 P_{CO2}\left(1-K_{eq2}\frac{P_{H2O}P_{CO}}{P_{CO2}P_{H2}}\right)}{\left(1+k_2\frac{P_{H2O}}{P_{H2}}+k_3 P_{H2}^{0.5}+k_4 P_{H2O}\right)}$</td><td>$r\left[\frac{mol}{kg_{cat}\cdot s}\right]$</td></tr>
<tr><td colspan="2">$\log_{10}K_{eq1} = \frac{3066}{T} - 10.592$</td><td colspan="2">$\log_{10}\frac{1}{K_{eq2}} = -\frac{2073}{T} + 2.029$</td><td rowspan="3">T [K]

P[bar]</td></tr>
<tr><td>$k_1 = 1.07\exp\left(\frac{36696}{RT}\right)$</td><td>$k_2 = 3453.38$</td><td colspan="2">$k_3 = 0.499\left(\frac{17197}{RT}\right)$</td></tr>
<tr><td colspan="2">$k_4 = 6.62E-11\left(\frac{124119}{RT}\right)$</td><td colspan="3">$k_5 = 1.22E10\exp\left(\frac{-94765}{RT}\right)$</td></tr>
</table>

4.4.5 Purification system

The purification system separates the light end components and water from the methanol product. In general, the system consists of a series of separator, flash drum and a distillation column. Similar to the compression system, a standardized industry approach was followed to design the purification system. By altering the process conditions (temperature and pressure), methanol can be isolated at high purity.

4.5 Process Simulation and Results

4.5.1 Process Description

Figure 4.2 shows the process flow diagram of the methanol plant. The entire flowsheet is developed with Aspen HYSYS v10 [53] using a combination of 3 different fluid packages. Majority of the process is modeled using Peng-Robinson. NRTL is selected for modeling the methanol-water liquid phase interactions in the purification system and ASME steam is used for modeling the steam generation and cooling water systems. The baseline production rate is 2095 ton/day, which is equivalent to the size of a commercial scale plant. The final product stream contains grade A methanol (99.9wt%), which can be used for various industrial purposes. The designed overall conversion of C_1 and CO_2 are 97% and 87%, respectively. In order to meet the designed specifications, the tri-reforming system must work synergistically with the water electrolysis system and deliver syngas at an optimum stoichiometric number (SN) of 2.0.

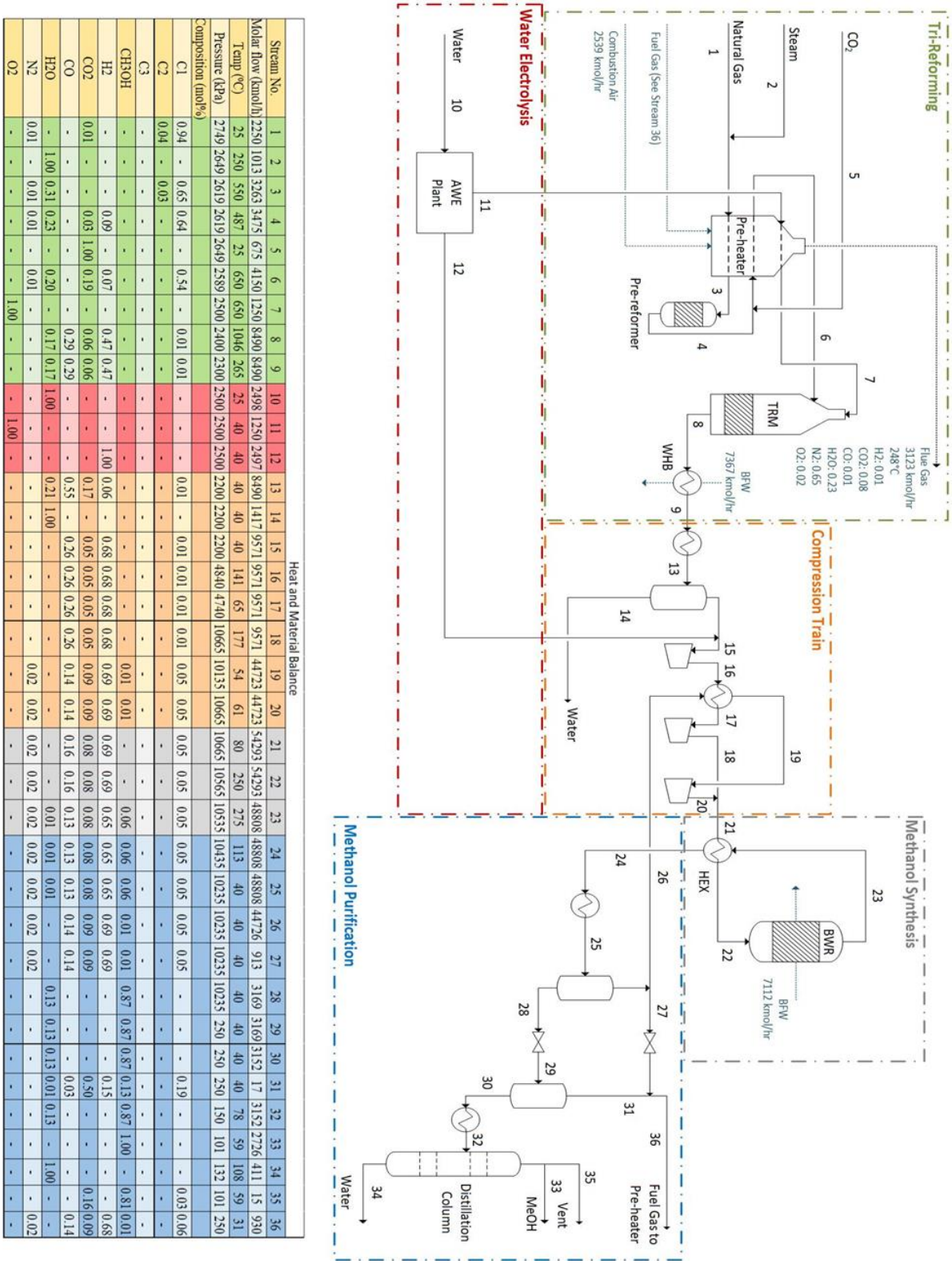

Heat and Material Balance																																		
Stream No.	1	2	3	4	5	6	7	8	9	10	11	12	13	14	15	16	17	18	19	20	21	22	23	24	25	26	27	28	29	30	31	32	33	34	35	36
Molar flow (kmol/h)	2250	1013	3263	3475	675	4150	1250	8490	8490	2498	1250	2497	8490	1417	9571	9571	9571	9571	44723	44723	54293	54293	48808	48808	48808	44726	913	3169	3169	3152	17	3152	2726	411	15	930
Temp (°C)	25	250	550	487	25	650	650	1046	265	25	40	40	40	40	40	141	65	177	54	61	80	250	275	113	40	40	40	40	40	40	40	78	59	108	59	31
Pressure (kPa)	2749	2649	2619	2619	2649	2589	2500	2400	2300	2500	2500	2500	2200	2200	2200	4840	4740	10665	10135	10665	10665	10565	10535	10435	10235	10235	10235	250	250	250	150	101	132	101	250
Composition (mol%)																																				
C1	0.94	-	0.65	0.64	-	0.54	-	0.01	0.01	-	-	-	0.01	-	0.01	0.01	0.01	0.01	0.05	0.05	0.05	0.05	0.05	0.05	0.05	0.05	-	-	-	0.19	-	-	-	0.03	0.06
C2	0.04	-	0.03	-	-	-	-	-	-	-	-	-	-	-	-	-	-	-	-	-	-	-	-	-	-	-	-	-	-	-	-	-	-	-	-	-
C3	-	-	-	-	-	-	-	-	-	-	-	-	-	-	-	-	-	-	-	-	-	-	-	-	-	-	-	-	-	-	-	-	-	-	-	-
CH3OH	-	-	-	-	-	-	-	-	-	-	-	-	-	-	-	-	-	-	0.01	-	-	-	0.06	0.06	0.06	0.01	0.87	0.87	0.87	0.13	0.87	1.00	-	0.81	0.01
H2	-	-	-	0.09	-	0.07	-	0.47	0.47	-	-	1.00	0.06	-	0.68	0.68	0.68	0.68	0.69	0.69	0.69	0.69	0.65	0.65	0.65	0.69	-	-	-	0.15	-	-	-	-	0.68
CO2	0.01	-	-	0.03	1.00	0.19	-	0.06	0.06	-	-	-	0.17	-	0.05	0.05	0.05	0.05	0.09	0.09	0.08	0.08	0.08	0.08	0.08	0.09	0.09	-	-	0.50	-	-	-	0.16	0.09
CO	-	-	-	-	-	-	-	0.29	0.29	-	-	-	0.55	-	0.26	0.26	0.26	0.26	0.14	0.14	0.16	0.16	0.13	0.13	0.13	0.14	0.14	-	-	0.03	-	-	-	-	0.14
H2O	-	1.00	0.31	0.23	-	0.20	-	0.17	0.17	1.00	-	-	0.21	1.00	-	-	-	-	-	-	-	-	0.01	0.01	0.01	-	-	0.13	0.13	0.13	0.01	0.13	-	1.00	-	-
N2	0.01	-	0.01	0.01	-	0.01	-	-	-	-	-	-	-	-	-	-	-	0.02	0.02	0.02	0.02	0.02	0.02	0.02	0.02	0.02	0.02	-	-	-	-	-	-	-	-	0.02
O2	-	-	-	-	-	-	1.00	-	-	-	1.00	-	-	-	-	-	-	-	-	-	-	-	-	-	-	-	-	-	-	-	-	-	-	-	-	-

Figure 4. 2 Process flow diagram of the methanol plant

At the tri-reforming system, pipeline spec. natural gas [33] (1) is fed together with superheated steam (2), post-combustion captured CO_2 (5) and oxygen (11) from water electrolysis. In this process, it is assumed that sulfur contents are negligible since the natural gas feed composition follows pipeline specifications. The multi-pass fired-heater initially heats the combined stream of natural gas and steam to 550ºC in order for the pre-reformer reactions to take place. The pre-reformed gas then gets combined with CO_2 and goes for a 2nd pass in the fired-heater to reach 650ºC before it is sent to the TRM reactor. Oxygen from water electrolysis is also pre-heated to 650ºC and sent to the TRM reactor. The total required duty of the fired heater is 42 MW which is met by burning the purged gas from the methanol synthesis loop. Both the pre-reformer and the TRM reactor are operated adiabatically and assumed to reach thermodynamic equilibrium over the catalyst Ni/Al_2O_3 [27]. In order to determine the required catalyst volume for the reactors, a conservative assumption of $3000h^{-1}$ gas hourly space velocity (GHSV) is applied [54]. The main difference is that for pre-reformer, the reaction is driven by the enthalpy of the inlet feed whereas for TRM reactor, the reactions are driven by the heat released from partial oxidation. In HYSYS, both of these reactors are modeled using the Gibbs reactor block in order to calculate the equilibrium compositions. The pre-reformer outlet composition shows that all of the C_{2+} hydrocarbons are consumed at the specified inlet temperature. As for the TRM reactor, the equilibrium composition shows that 97% of the C_1 and 39% of the CO_2 are converted. Reactor effluent (8) consists of mostly syngas in the $CO/CO_2/H_2$ molar ratio of 0.29/0.06/0.47. This is equivalent to a stoichiometric number (SN) of 1.2, which indicates that additional H_2 is needed for methanol synthesis. Temperature of the reactor effluent is 1046ºC. Heat energy is recovered by cooling the

reactor effluent down to 265ºC through a waste heat boiler (WHB) to generate high-pressure steam (HPS).

The water electrolysis system is designed to supply O_2 and H_2 for the main process. The main component of this system is a set of 15 modules of tkUCE 20 MW AWE. The entire system has a total power consumption of 300 MW. Each AWE module is operated at 66.6% efficiency. Demineralized water (10) is initially fed to the 15 modules. With carbon-free electricity, the water is split into O_2 (11) and H_2 (12) and the gases are collected based on the designed specification of 99.95mol% purity. Since carbon-free electricity is often derived from renewable energy source such as wind and solar, temporary storage vessels are necessary to ensure that the plant can be operated at steady state. Compressors will be included in the system to deliver the produced gas at 2500 kPa. In HYSYS simulation, a simplified model is developed using a conversion reactor and a component splitter.

H_2 from water electrolysis is added to the TRM reactor effluent to create the optimal SN of 2.0. The syngas (15) is fed through a two-staged centrifugal compressor with a compression ratio of 2.2 per stage. An inter-stage cooler is used to prevent temperature from going above 200 ºC during the second stage compression. In addition to syngas compression, recycled gas (19) from the purification system is also sent here for re-compression. The recycling ratio (stream 19/stream 15) is 4.67. The recycled gas compressor has a compression ratio of 1.05. All compressors designed in the simulation are centrifugal type and has a polytropic efficiency of 80%. The total power consumption of the compression system is 19.3 MW. Together, the syngas and recycled gas are

combined (21) and delivered to the methanol synthesis system at a pressure of 10,670 kPa.

The combined feed gas (22) is preheated to 250 ºC through a feed gas/effluent heat exchanger before introduced to the BWR. The BWR is modelled using a plug flow reactor (PFR) with a heterogeneous reaction set (LHHW). The reactor contains 2700 tubes with uniform diameters and lengths of 0.035 m and 7.0 m, respectively. The total volume of the reactor tube side is 18 m^3. Inside each tube contains the commercial $Cu/ZnO/Al_2O_3$ spherical catalyst pellets with an average diameter of 0.005 m. These pellets have a bulk density of 1140 kg/m3 and make up 60% of the total reactor volume. During operations, the BWR is oriented vertically with the feed gas introduced at the bottom. Temperature is controlled by injecting 128 t/h of high-pressure saturated water on the shell side of the BWR. 61MW of heat energy is absorbed from the reactions to generate high-pressure steam. The BWR components' molar concentration and temperature profiles are shown in Figure 4.3. In a single pass, 15.7% of H_2, 27.3% of CO and 9.0% of CO_2 are converted. The BWR effluent (23) at 275 ºC is cooled against the reactor feed gas stream down to 113 ºC (24) before it is sent to the purification system.

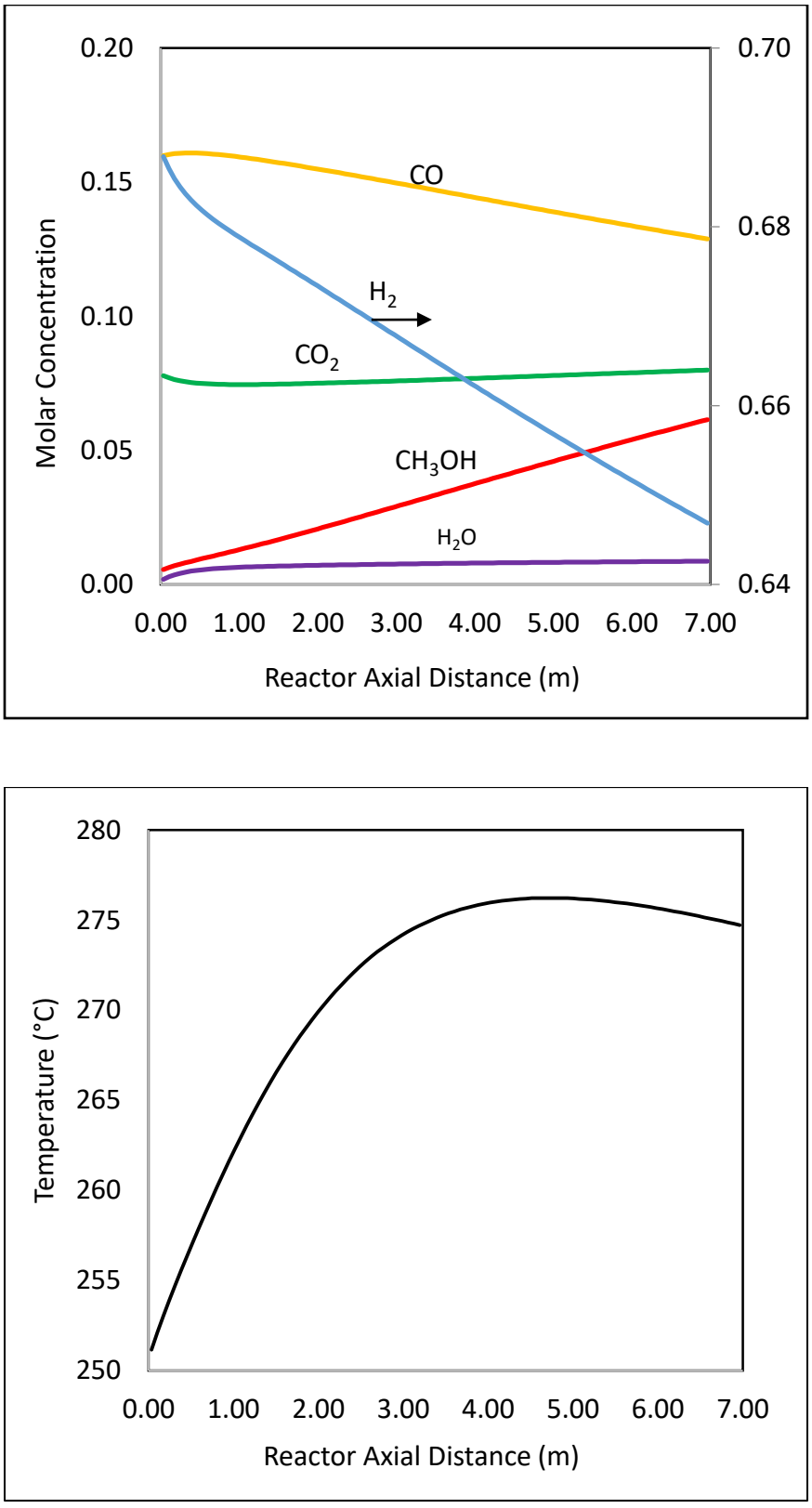

Figure 4. 3 BWR molar concentration profile (top) and temperature profile (btm.)

At the purification system, the BWR effluent is initially cooled down to 40ºC (25) and sent to the separator. 96% of methanol and 98% of water is condensed and separated (28) from the unreacted gas. To prevent inert concentration build-up in the recycle loop, 98% of the unreacted gas (26) is sent back for re-compression while the remainder 2% (27) is purged and sent to the pre-heater as fuel gas (36). Downstream of the two-phase separator, a throttling valve is used to reduce the pressure down to 250 kPa (29). Then a flash drum is used to separate most of the remaining dissolved gas in the stream (31). The remaining methanol and water mixture (30) is then preheated to 78ºC (32) and sent to the distillation column for final separations. The distillation column has 22 stages, a partial reboiler and a partial condenser. The required heating duty of the reboiler is 65.0 MW, which is supplied by the high-pressure steam generated in the earlier processes. The required cooling duty of the condenser is 64.1 MW, which is supplied by 3,688 t/h of cooling water. The feed is introduced at stage 12, water (34) is separated to the bottom and methanol (33) is collected at the top. A vent gas stream (35) is also introduced at the top of the partial condenser to separate trace amounts of impurities from the methanol product. The molar concentration and temperature profile of the distillation column is shown in Figure 4.4. Overall, the distillation column delivers methanol at 99.5% recovery and 99.9wt% purity.

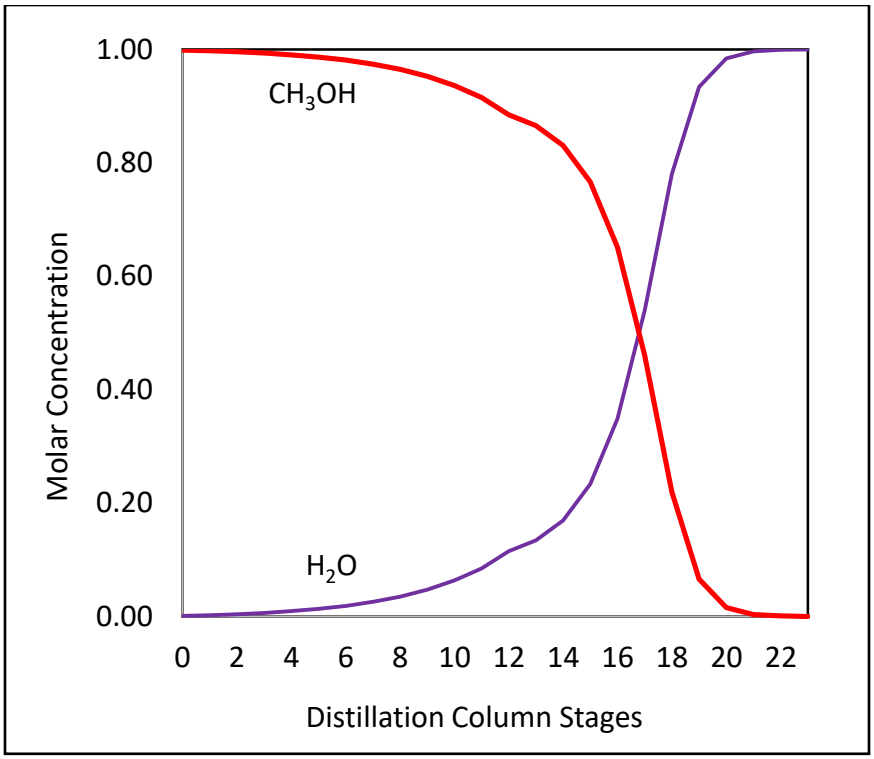

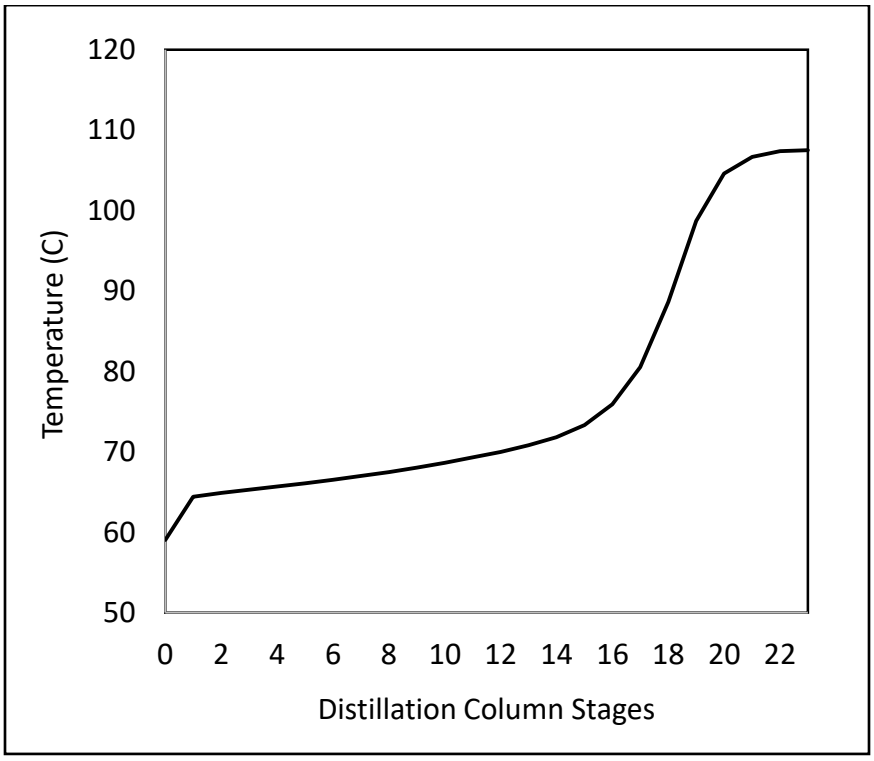

Figure 4. 4 Column molar concentration profile (top) and temperature profile (btm.)

4.5.2 Net energy efficiency

The net energy efficiency of this process is defined as the ratio between total energy output and total energy input:

$$\eta_{\text{Process}} = \frac{\text{GHV}_{\text{MeOH}}}{\text{GHV}_{\text{NG}} + \text{Q}_{\text{Process}}}, \text{Q}_{\text{Process}} = \text{Q}_{\text{Electricity}} + \text{Q}_{\text{Heat}} \quad (30)$$

In this study, the total energy output is the gross heating value of methanol (GHV_{MeOH}) calculated using the higher heating value (HHV) property. At full plant capacity, GHV_{MeOH} is 546 MW. On the other hand, the total energy input includes a combination of electricity, heat and natural gas consumptions. The gross heating value of consumed natural gas (GHV_{NG}) is 566 MW. The rest of the energy input coming from electricity and heat consumptions in the plant are summarized in Table 4.2. As previously discussed, heat energy is recovered from the waste heat boiler (WHB) and boiling water reactor (BWR) by generating high pressure steam. Majority of this steam is used to provide heating duty for the distillation column reboiler. Another portion is consumed as reactants in the TRM reactor. The rest of the excess steam is not considered in the energy efficiency calculations, but can be used for various on-site heating purposes.

The net energy efficiency of the baseline process was determined to be 62%. Figure 4.5 shows a comparative study with other processes reported in literatures. While the baseline process implemented in this study is more energy efficient compared to direct CO_2 hydrogenation, there is still a considerable gap from the commercial natural gas process. One of the key bottlenecks of the current design is the efficiency of water electrolysis, which has significant potentials for improvements. In addition, further

developments can still be made on the process design by carrying out energy optimizations to reduce the overall energy consumptions.

Table 4. 2 Electricity, heat consumptions of each subsystem in the plant

Plant Subsystems	Energy Consumptions (+) and Productions (-)	
	Electricity (kW)	Heat (kW)
Water Electrolysis System:		
20-MW AWEs x 15	300000	-
Tri-Reforming System:		
TRM Pre-heater Air Blower	967	-
Waste Heat Boiler	-	-63360
Steam Consumption (Gen. Energy)	-	13650
Compression System:		
Syngas Feed 1st Stage Compressor	7936	-
Syngas Feed 2nd Stage Compressor	8971	-
Recycle Gas Compressor	2363	-
Methanol Synthesis System:		
Boiling Water Reactor	-	-61000
Boiler Feed Water Circulation Pump	23	-
Make-Up Water Pump	28	-
Purification System:		
Distillation Column Reboiler	-	64760
Cooling Water Circulation Pump	295	-
Net Energy Consumption:		
	320288	-45950

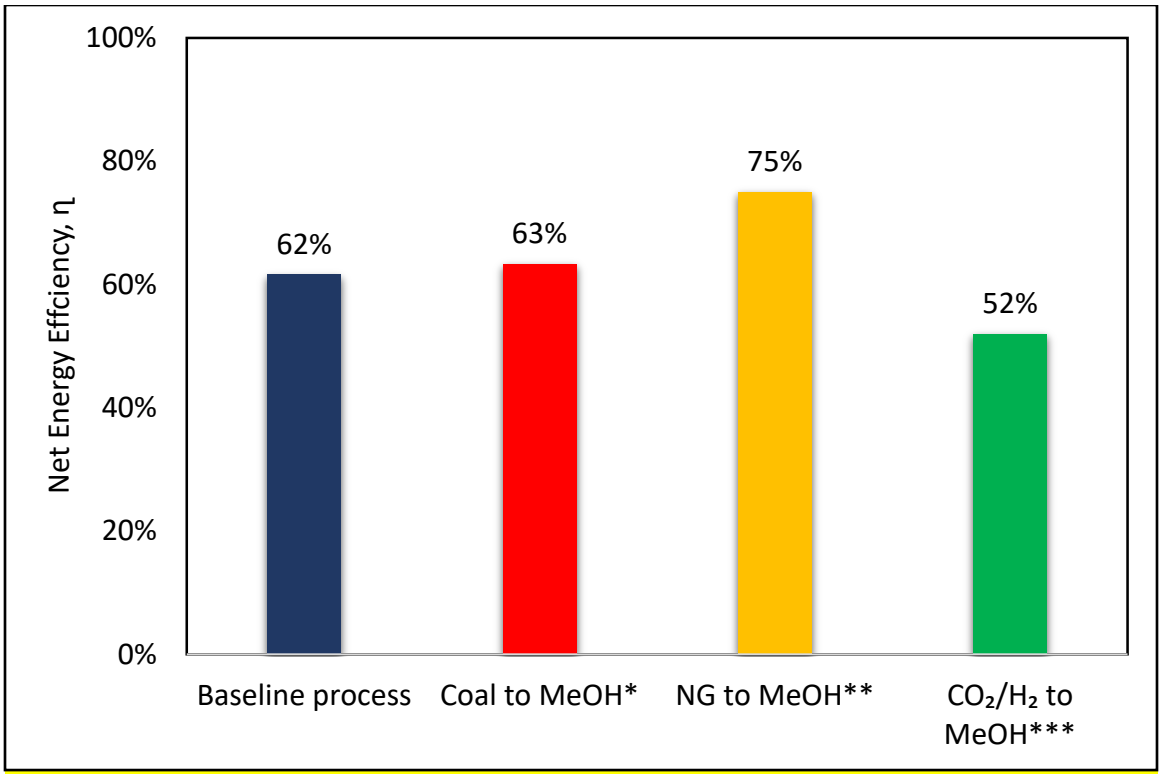

Figure 4. 5 Net energy efficiency comparison of various methanol synthesis processes. *The coal to methanol process is based on the gasification technology simulated using Pro/II [55]. **The natural gas to methanol process is based on the conventional steam reforming technology [8]. ***The CO_2/H_2 to methanol process is based on direct CO_2 hydrogenation where H_2 comes from water electrolysis [37].

4.6 Environmental Impact Evaluation

The two species of greenhouse gases considered in this project are CO_2 and CH_4. The metrics used for determination of 100-year global warming potential (GWP_{100}) are in accordance with IPCC 2014 AR5 [56]. Figure 4.6 shows the defined system boundary of this study, which include direct emissions from the methanol plant and indirect emissions from natural gas extraction and processing, electricity generation and heat generation. In order to estimate the indirect emissions, the following data were retrieved from an LCA analysis performed by Kim et al. [57]:

1. Conventional electricity generation is 0.407 kg CO_2 eq./kWh

2. Conventional heat generation is 0.233 kg CO_2 eq./kWh

3. Natural gas extraction and processing is 0.178 kg CO_2 eq./kg NG

The total emitted CO_2 is then calculated based on the following equation:

$$\mathrm{nCO_2, emitted} = \mathrm{nCO_2, direct} + \mathrm{nCO_2, indirect} \quad (41)$$

A comparative case study was conducted to evaluate the GWP_{100} differences between the baseline process configuration and the conventional methanol production process. Three different cases were considered as follows:

- Case 1: Conventional methanol production using natural gas and steam. This process consists of three major steps: steam methane reforming, methanol synthesis and product purification. The emission data for this process were retrieved from literature [57].
- Case 2: Baseline process configuration using electricity from the power grid. It is assumed that energy source for electricity generation is based on the US fuel mix of 2009 [57], [58].
- Case 3: Baseline process configuration using electricity from carbon-free generation processes only (i.e. wind, solar and nuclear) where zero emissions can be assumed.

The results from the case study are shown in Figure 4.7. In this study, it is assumed that CO_2 fed to the process as raw material is counted as negative emissions. The

conventional process (case 1) emits GHG from all sources defined in the system boundary and the total GWP_{100} is 0.67 $tCO_2eq./tMeOH$. On the other hand, the baseline process configuration (case 2 and case 3) use CO_2 as raw material, require less natural gas and does not require external heat supply. Nevertheless, despite having these advantages, the overall GWP_{100} for the baseline process configuration would still be higher than the conventional process if the electricity consumption is drawn directly from the power grid. In order to realize the target of net negative carbon emissions, electricity supply must be entirely based on carbon-free generation technologies. It was determined that a GWP_{100} of -0.14 $tCO_2eq./tMeOH$ can be achieved if the baseline process uses carbon-free electricity. In comparison to the conventional methanol process, this is about 570,000 ton of CO_2 mitigated annually when the plant is operating at full capacity.

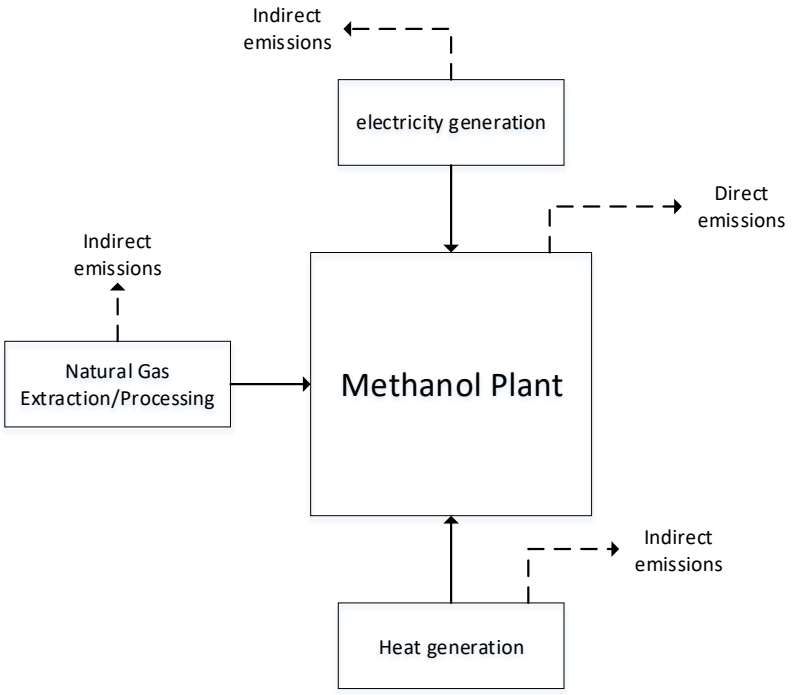

Figure 4. 6 Defined system boundary for direct and indirect GHG emissions

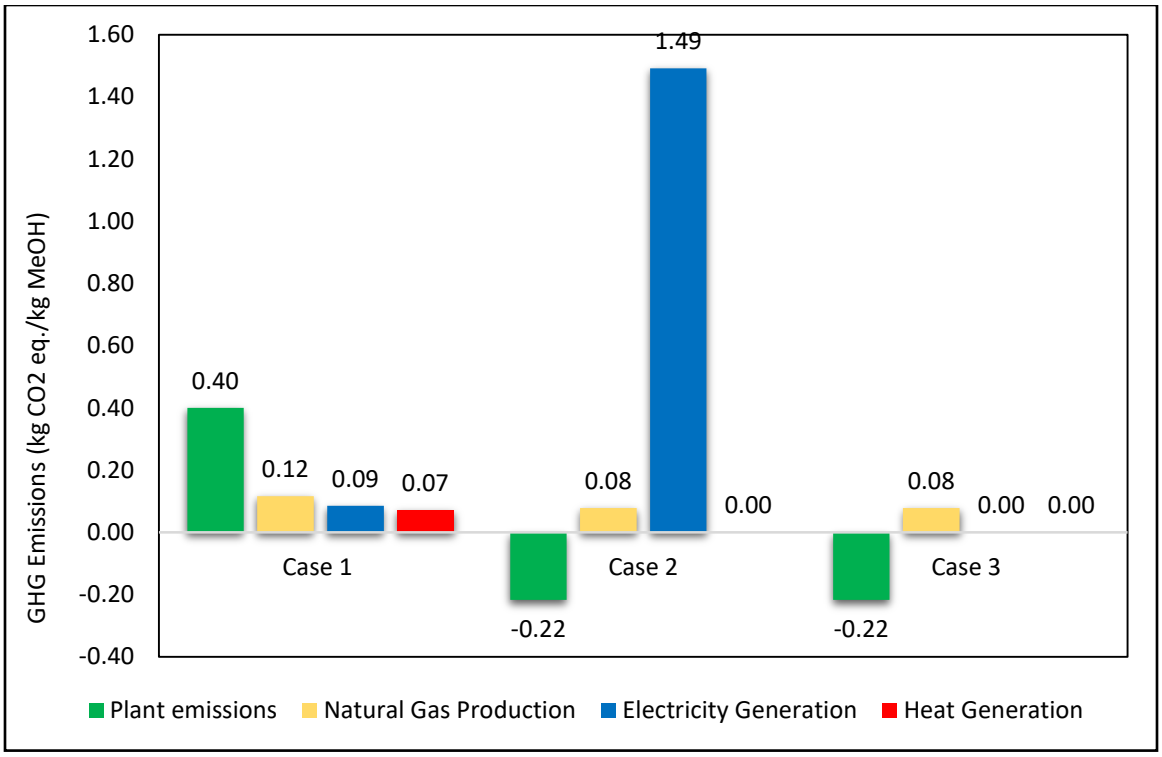

Figure 4. 7 GHG emissions of the three different cases considered in this study

4.7 Economic Evaluation

An economic study was conducted to determine the financial feasibility under various market conditions. Results from the process simulation flowsheet were used to estimate the capital expenditure (CAPEX), operating expenditure (OPEX) and revenue. Based on these estimations, a discounted cash flow (DCF) model was developed to determine the net present value (NPV) of this process. A sensitivity analysis was performed on the DCF model to determine the impact of different variables on the NPV.

4.7.1 Economic Assumptions

The main economic assumptions used for this study are shown in Table 4.3. This is a grass roots plant based in North America. The specific location is set in the Gulf Coast, Texas, United States for favorable economic conditions such as market access, utilities prices and corporate income tax. This project is set to initiate in 2018 with 3 years for construction and 1 year for commissioning and start-up (C&SU). During the construction phase, it is assumed that 1st and 2nd year will use 50% of the CAPEX and the 3rd year will use the remainder CAPEX. Once construction reaches 100% completion, operations can be initiated. The start-up year is assumed to reach 50% of the plant capacity and the following years are assumed to reach full plant capacity. The life expectancy of this project is assumed to be 20 years, which is consistent to other similar processes and technologies. In order to account for the time value of money, an annual discount rate of 8.0% was applied. On top of that, an inflation rate of 1.9% retrieved from the US Bureau of labor statistics in 2018 was assumed over the project lifespan [59]. In terms of asset depreciation, a straight line method was adopted with 20% salvage value. The plant asset is assumed to be liquidated after 20 years of operation. For pre-design estimates, the working capital of this project was assumed to be 15.0% of fixed capital expense, which is a typical value for traditional chemical plant operation [60], [61]. In order to account for plant turnarounds and unplanned outages, an on-stream factor of 91% is assumed (The equivalence of 7,992 operating hours per year). The revenue generated from the production and sales of methanol is subject to a 21.0% corporate income tax for the state of Texas [62].

Table 4. 3 List of baseline economic assumptions for this project investment

Referenced Year of Project Initiation	2018
Project Life	20 years
Project Location	Texas, US
Inflation rate	1.9%
Depreciation type	Straight line with 20% salvage value
Income tax	21.0%
Annual discount rate, i	8.0%
Working capital (WC)	15.0% of fixed capital
Construction period	3 years
Start-up (C&SU) period	1 Year
Operating hours per year	7992 hours (91% on-stream factor)

4.7.2 Capital Expenditure (CAPEX)

The steps followed for the determination of CAPEX are mostly in accordance with "Chemical Engineering Process Design and Economics: A Practical Guide" handbook [61]. The main project expenses are associated with the plant bare module cost, which includes the purchase and installation of all process equipment within the battery limit. Cost data were retrieved for standardized process equipment and adjusted based on size, material of construction, pressure rating and the Chemical Engineering Plant Cost Index (CEPCI) of 2018 [63]. For water electrolysis system and tri-reforming system, price estimations had to be obtained from specific vendors [35], [64], because specialized process equipment were used. The offsite facilities, project contingency and working capital were considered based on the following:

- Offsite facilities: 30% of plant bare module. This includes any auxiliary buildings, product storage tanks, chemical supplies and miscellaneous utilities.
- Project contingency: 30% of plant bare module. This accounts for unforeseen expenses, unexpected delays, disruptive weather etc.
- Working capital: 15% of fixed capital (See section 4.6.1). The fixed capital cost is the summation of plant bare module, offsite facilities and project contingency.

The total CAPEX of this project is calculated to be US$774 million. Figure 4.8 shows the break-down of CAPEX associated with each major portion of project investment. While offsite facilities, project contingency and working capital are fixed percentages based on the main project expenses, CAPEX reduction measures can be considered for each of the plant subsystems. Among the subsystems, water electrolysis accounts for the most significant portion of capital investment (about 62% of the plant bare module investment).

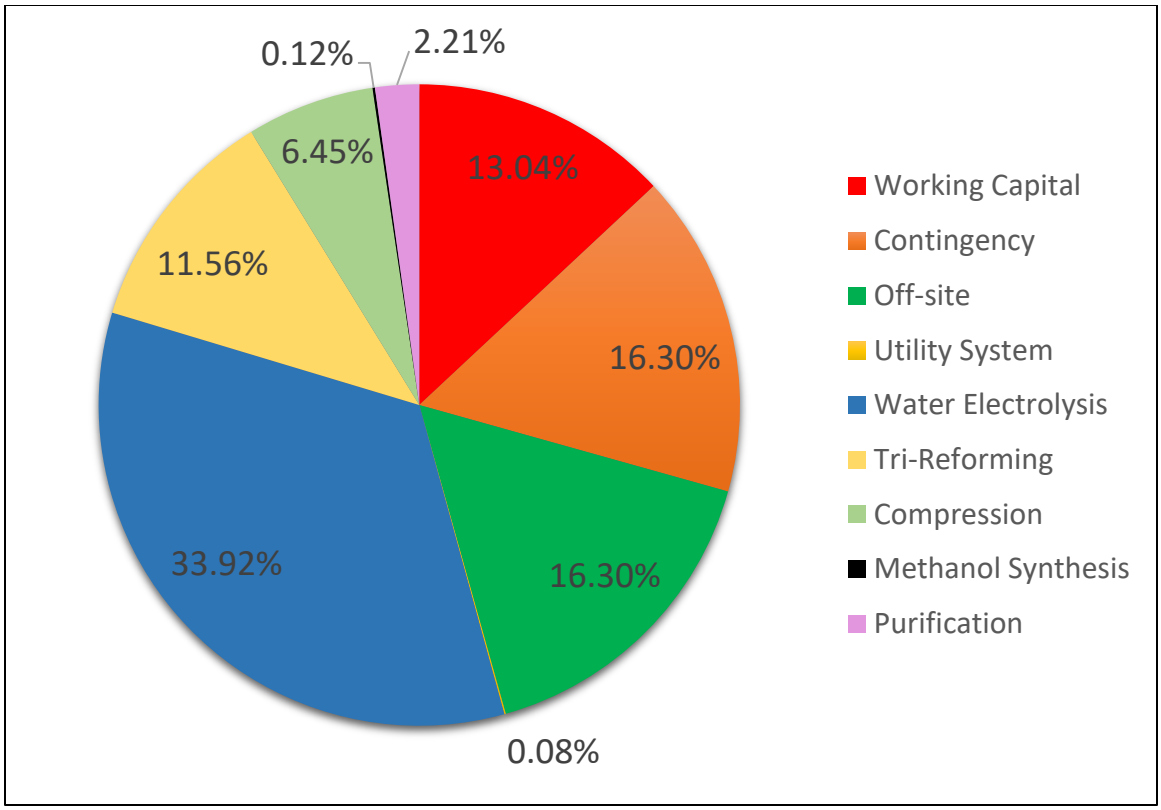

Figure 4. 8 Distribution of CAPEX for the methanol plant

4.7.3 Operating Expenditure (OPEX)

The annual OPEX can be divided into direct and indirect expenses. Direct expenses include raw materials, utilities, catalysts, operating labor, supervision, maintenance, supplies, laboratory charges, patents and royalties. The indirect expenses include overhead, local taxes and insurance. The prices of raw materials and utilities used in this study are listed in Table 4.4. The catalysts used during plant operation include Ni/Al_2O_3 and Cu/ZnO and their price information were retrieved from NREL [65]. Since catalysts degrade over time, they are assumed to be replaced every 5 years. Based on the size and scale of this methanol plant, it was estimated that a total of 30 plant operators are required for daily operations and the annual salary for each operator is US$62,380

according to the US Bureau of Labor Statistics [66]. The rest of the operating expenses were calculated as follows: supervision is 10% of operating labor costs, maintenance is 2% of fixed capital, plant supplies is 10% of maintenance, laboratory charges is 10% of operating labor, patents and royalties is 2% of direct expense, plant overhead is 50% of operating labor, supervision and maintenance, local taxes is 2% of fixed capital and insurance is 1% of fixed capital. The annual OPEX of this project is calculated to be US$263 million/yr. Figure 4.9 shows that OPEX distribution for this project is dominated by the cost of electricity consumption at 54.2%. This is an expected outcome since the water electrolysis system along consumes about 300 MW of electricity.

Table 4. 4 Raw materials and utilities prices considered in this project

Raw Materials	
Natural Gas (US$/mmBtu) [67]	3.17
CO_2 (US$/ton) [34]	86.40
Water (US$/$m^3$) [61]	5.95
Utilities	
Electricity (US$/kWh) [68]	0.06
Cooling Water (US$/$m^3$) [61]	0.05

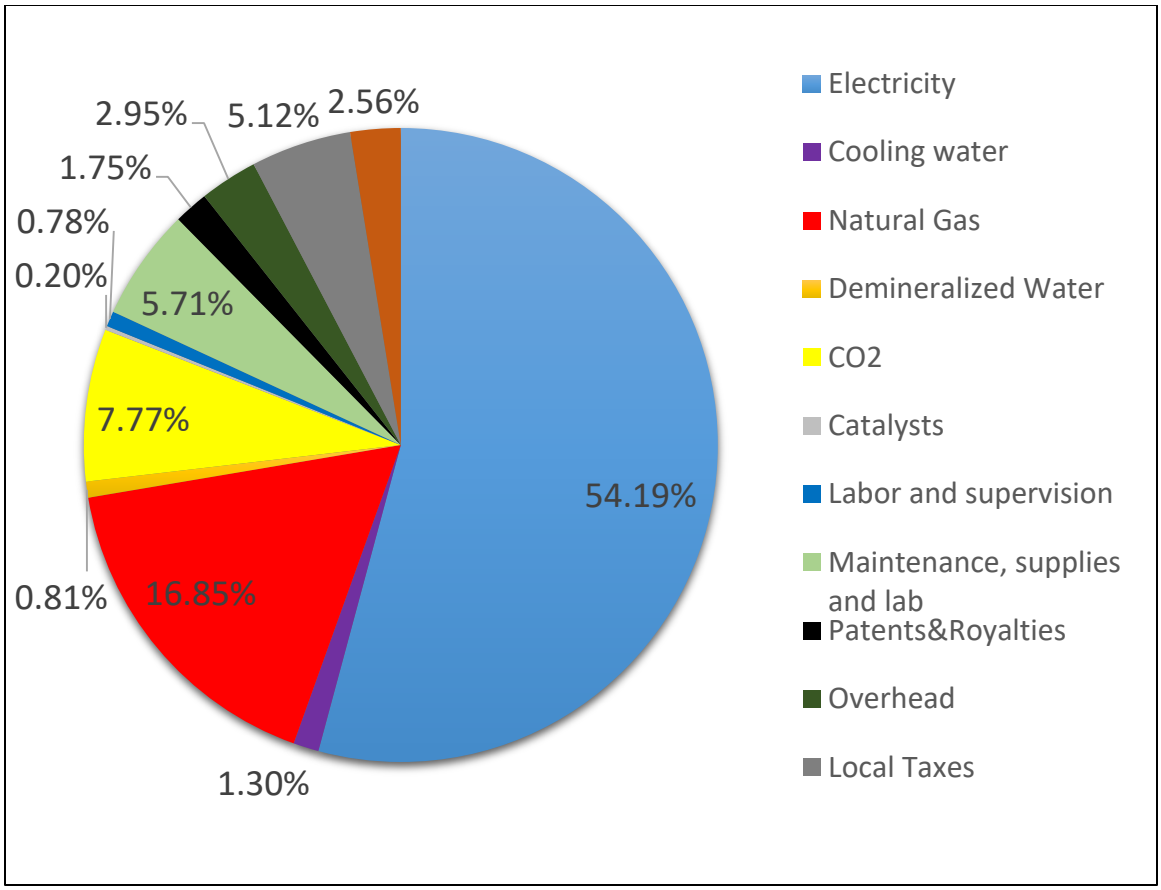

Figure 4. 9 Distribution of OPEX for the methanol plant

4.7.4 Revenue

Based on the current design considerations, methanol is the only source of revenue for this project. From the historical data, it can be observed that the price of methanol is highly volatile. For the purpose of this study, US$493.25/t was assumed based on the average methanol price of 2018 according to Methanex [69]. When the plant is operating at full capacity, the annual product sales revenue generated is US$343 million.

4.7.5 Economics Summary

A DCF model is developed incorporating all results and assumptions. The steps followed in the DCF analysis are presented in Appendix D. Figure 4.10 illustrates the net cash flow of this project over the entire lifespan from construction to full-scale operation. It is determined from DCF that this project will have a net payout time (NPT) of 19.8 years and a positive net present value (NPV) of US$11.4 million after 20 years of operation. The internal rate of return (IRR) for this project is at 8.17%. Table 5.3 provides a summary of the economic performance of this project. In comparison to direct CO_2 hydrogenation [8], the economic feasibility of this process is far superior.

Table 4. 5 Economic Results Summary

Total capital expenditure	US$774 million
Total operating expenditure	US$263 million/yr.
Total product sales revenue	US$343 million/yr.
Net payout time (NPT)	19.8 years
Net present value (NPV)	US$11.4 million
Internal rate of return (IRR)	8.17%

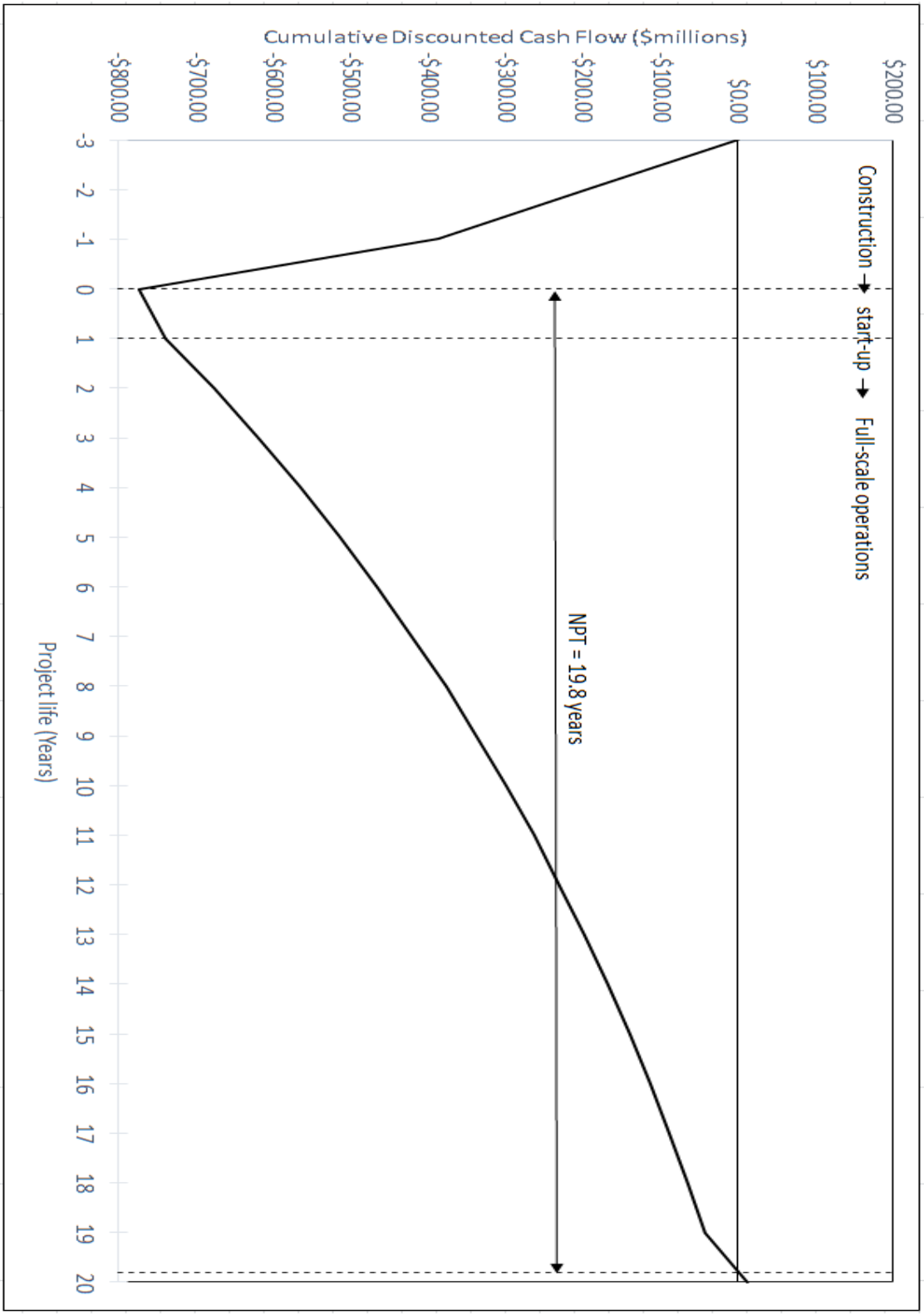

Figure 4. 10 Cumulative discounted cash flow of this project over 20 years of operation

4.7.6 Sensitivity Analysis

A sensitivity analysis is performed to determine the relative impacts of raw materials, utilities and product prices on the NPV. The prices of each variable are deviated by +/- 20% from their baseline values and the respective impacts are reflected in the tornado diagram in Figure 4.11. The order of significance is shown from the top (selling price of methanol) to bottom (purchase cost of demineralized water). Based on the current model, the breakeven selling price of methanol is US$491/t which is lower than the average price of 2018. However, a drop of only US$2/t would take this project to an unprofitable condition.

Several areas can be considered to improve the economic feasibility of this project. One of the key driving factors is process improvements related to water electrolysis. Further R&D efforts focused on improving the energy efficiency can lead to reductions in both electricity consumption and equipment purchase cost. Another consideration for cost reduction is through further developments in clean energy processes. Progress in wind, solar and nuclear energy sectors can reduce the cost of carbon free electricity generation down to a more affordable level. Lastly, improvements in carbon capture processes can also provide additional savings. The current price of CO_2 capture is US$86.40/t using the amine absorption technology from a post combustion capture plant. However, with the new integrated gasification combined cycle (IGCC) plants, the cost of CO_2 capture can be as low as US$11.00/t [70].

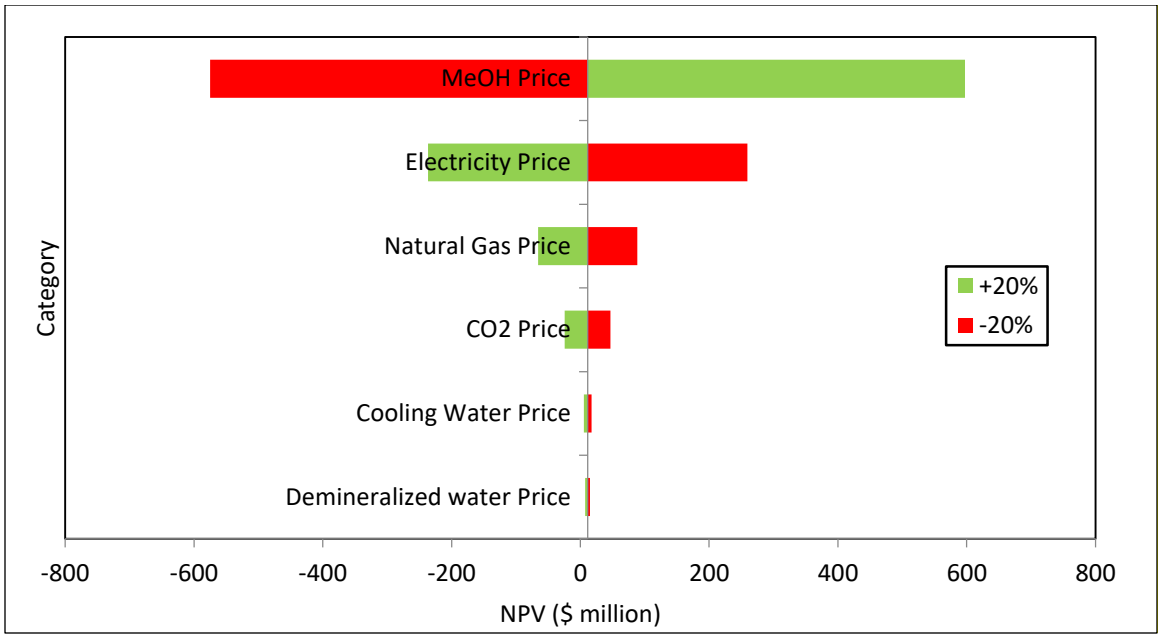

Figure 4. 11 Sensitivity analysis using the tornado diagram

4.8 Conclusions and Recommendations

Methanol production with CO_2 utilization can be a sustainable pathway to meet future global energy demands. In order to overcome the technical and economic challenges of direct CO_2 hydrogenation, this study investigated the combined state-of-the-art technologies of water electrolysis with tri-reforming for methanol production. The primary objective was reached by the conceptual design of a commercial scale methanol plant with net negative carbon emissions. Project feasibility was then evaluated based on the technical, environmental and economic performance.

The major steps took in process design consisted of technology selections and flowsheet developments using Aspen HYSYS v10. The heat and material balance data obtained from simulation results were used to perform equipment sizing, reactor conversions, and net energy efficiency calculations. Through the combined processes of tri-reforming,

water electrolysis and methanol synthesis, the overall conversions of CH_4 and CO_2 are 97% and 87%, respectively. The net energy efficiency of this process was determined to be 62%, which is distinctively higher in comparison to direct CO_2 hydrogenation.

The environmental impact of this project was evaluated by considering the GHG emissions of CO_2 and CH_4. The method of calculation included both direct emissions from the methanol plant and indirect emissions from the consumption of raw materials and utilities. Results have shown that if carbon-free electricity is used, this process is capable of reaching net negative carbon emissions of -0.14 $tCO_2eq./tMeOH$. In comparison to a traditional methanol plant, this is a net reduction of CO_2 emissions by 570,000 tons annually.

The economic feasibility of this project was evaluated with DCF analysis using standard project assumptions. The estimated CAPEX and OPEX of this project are US$774 million and US$263 million/yr., respectively. From the DCF model, it was determined that a positive NPV of US$11.4 million can be achieved after 20 years of operation. From the sensitivity analysis, it was shown that the selling price of methanol has the highest impact on NPV and the breakeven point is at US$491/ton. With better technologies available for water electrolysis, electricity generation, and CO_2 capture, the economics of this project is anticipated to reach much greater improvements.

Acknowledgement

The authors would like to extend their gratitude to the Natural Sciences and Engineering Research Council (NSERC) of Canada for funding this research, through its Industrial Research Chairs (IRC) program.

Chapter Five: **Conclusion and Recommendations**

5.1 Conclusions

The "Methanol Economy" is a promising concept that ensures the long term stability of global energy supply. The main challenge is to figure out a cost-effective solution in producing renewable methanol. Direct CO_2 hydrogenation demonstrated great potentials in terms of sustainability and environmental benefits. However, the high costs of this process may prevent it from further large scale implementations by the industry. To overcome the challenges of direct CO_2 hydrogenation, this study investigated the combination of tri-reforming of methane (TRM) and water electrolysis for methanol synthesis.

Through process simulation and economic analysis, this study was able to demonstrate several advantages of combining TRM with water electrolysis. One of the main advantages is that an increased amount of CO_2 can be converted to syngas without concerns on the stoichiometric number (SN). Since syngas produced by TRM on its own would typically be deficient in H_2 for methanol synthesis, but with the addition of H_2 from water electrolysis, this problem can be effectively alleviated. The other main advantage is that O_2 from water electrolysis can be fully utilized in TRM. In direct CO_2 hydrogenation, O_2 from water electrolysis is typically considered a by-product and is vented to the atmosphere. By using the O_2 for partial oxidation reactions in TRM, this eliminates the need for an air separation unit (ASU), thereby effectively reducing the capital and operating expenses. With these advantageous, the economic feasibility of this process has significantly improved in comparison to direct CO_2 hydrogenation. Using

economic parameters from 2018, this design is capable to achieve a positive NPV of $11.4 million with a breakeven methanol price of $491/t.

5.2 Recommendations

For the continuation and further expansion of this conceptual design, the author would like to make the following recommendations as future steps.

5.2.1 Experimental evaluation

The combination of TRM with water electrolysis is only a theoretical concept. Before the commercialization of this process, it is recommended to perform additional testing through laboratories and pilot plants. The idea of performing tests is to identify any potential operating concerns. For instance, if the water electrolysis process is operated based on solar or wind energy, then the whole process would be subject to a high degree of fluctuation. It is important to analyze the impact of process fluctuations so that adequate control measures can be implemented.

5.2.2 Further cost reduction measures

In order for this process to gain further attractions within the methanol industry, it is highly recommended to look for additional steps to reduce costs. In the process, the main costs are associated with the water electrolysis process, which accounted for roughly 34% of CAPEX and 54% of OPEX. With further improvements on water electrolysis energy efficiency, both the CAPEX and OPEX can be significantly reduced.

References

[1] "How Methanol is Used | Methanex Corporation." [Online]. Available: https://www.methanex.com/about-methanol/how-methanol-used. [Accessed: 12-Mar-2020].

[2] "OECD iLibrary | World Energy Outlook 2014." [Online]. Available: https://www.oecd-ilibrary.org/energy/world-energy-outlook-2014_weo-2014-en. [Accessed: 24-Feb-2020].

[3] G. A. Olah, "Towards Oil Independence Through Renewable Methanol Chemistry," pp. 104–107, 2013.

[4] I. ~ Nigo Capell An-P Erez, M. Mediavilla, C. De Castro, O. Carpintero, and L. J. Miguel, "Fossil fuel depletion and socio-economic scenarios: An integrated approach," *Energy*, pp. 641–666, 2014.

[5] "Alternative Fuels Data Center - Fuel Properties Comparison." [Online]. Available: https://afdc.energy.gov/fuels/fuel_comparison_chart.pdf. [Accessed: 21-Mar-2020].

[6] PubChem, "METHANOL | CH3OH," *National Center for Biotechnology Information*, 2004. [Online]. Available: https://pubchem.ncbi.nlm.nih.gov/compound/methanol#section=Top. [Accessed: 04-Mar-2020].

[7] G. A. (George A. Olah, A. Goeppert, and G. K. S. Prakash, *Beyond oil and gas : the methanol economy*. Wiley-VCH, 2009.

[8] G. Bozzano and F. Manenti, "Efficient methanol synthesis : Perspectives , technologies and optimization strategies," *Prog. Energy Combust. Sci.*, vol. 56, pp. 71–105, 2016.

[9] J. Matthey, P. O. Box, and B. Avenue, "Methanol Production – A Technical History," no. 3, pp. 172–182, 2017.

[10] "How is Methanol Produced|Methanol Institute." [Online]. Available: https://www.methanol.org/methanol-production/. [Accessed: 24-Feb-2020].

[11] R. Fukui, C. Greenfield, K. Pogue, and B. van der Zwaan, "Experience curve for natural gas production by hydraulic fracturing," *Energy Policy*, vol. 105, pp. 263–268, Mar. 2017.

[12] M. Bertau, H. Offermanns, L. Plass, F. Schmidt, and W. Hans Jurgen, *Methanol: The Basic Chemical and Energy Feedstock of the Future*. 2014.

[13] X. Xu, Y. Liu, F. Zhang, W. Di, and Y. Zhang, "Clean coal technologies in China based on methanol platform," *Catal. Today*, vol. 298, pp. 61–68, 2017.

[14] "Projects: Emissions-to-Liquids Technology — CRI - Carbon Recycling

International." [Online]. Available: https://www.carbonrecycling.is/projects#project-goplant. [Accessed: 26-Feb-2020].

[15] F. Pontzen, W. Liebner, V. Gronemann, M. Rothaemel, and B. Ahlers, "CO2-based methanol and DME - Efficient technologies for industrial scale production," *Catal. Today*, vol. 171, no. 1, pp. 242–250, 2011.

[16] P. J. A. Tijm, F. J. Waller, and D. M. Brown, "Methanol technology developments for the new millennium," *Applied Catalysis A: General*, vol. 221, no. 1–2. pp. 275–282, 2001.

[17] Kim Aasberg-Petersen, Charlotte Stub Nielsen, Dybkjær, and Jens Perregaard, "Large Scale Methanol Production from Natural Gas," *Haldor Topsoe*, pp. 1–14, 2013.

[18] F. Schuth and J. Weitkamp, *Handbook of Heterogeneous Catalysis*, vol. 5. WILEY-VCH, 1999.

[19] S. A. Bhat and J. Sadhukhan, "Process intensification aspects for steam methane reforming: An overview," *AIChE J.*, vol. 55, no. 2, pp. 408–422, Feb. 2009.

[20] J. P. Lange, "Methanol synthesis: A short review of technology improvements," *Catal. Today*, vol. 64, no. 1–2, pp. 3–8, Jan. 2001.

[21] J. M. Lavoie, "Review on dry reforming of methane, a potentially more environmentally-friendly approach to the increasing natural gas exploitation," *Front. Chem.*, vol. 2, no. NOV, pp. 1–17, 2014.

[22] M. K. Nikoo and N. A. S. Amin, "Thermodynamic analysis of carbon dioxide reforming of methane in view of solid carbon formation," *Fuel Process. Technol.*, 2011.

[23] R. Luque and J. G. Speight, *Gasification for Synthetic Fuel Production: Fundamentals, Processes and Applications*. Elsevier Ltd, 2014.

[24] J. Oakey, *Fuel Flexible Energy Generation: Solid, Liquid and Gaseous Fuels*. Elsevier Inc., 2015.

[25] J. Zhu, D. Zhang, and K. D. King, "Reforming of CH4 by partial oxidation: Thermodynamic and kinetic analyses," *Fuel*, 2001.

[26] A. Goeppert, G. K. S. Prakash, and G. A. Olah, "Recycling of carbon dioxide to methanol and derived products – closing the loop," vol. 43, no. 23, 2014.

[27] J. G. Speight, *Gasification of Unconventional Feedstocks*. 2014.

[28] M. H. Halabi, M. H. J. M. de Croon, J. van der Schaaf, P. D. Cobden, and J. C. Schouten, "Modeling and analysis of autothermal reforming of methane to hydrogen in a fixed bed reformer," *Chem. Eng. J.*, vol. 137, no. 3, pp. 568–578, 2008.

[29] P. Dahl, T. Christensen, S. Winter-Madsen, and S. King, "Proven autothermal

reforming technology for modern large- scale methanol plants," *Proven autothermal reforming Technol. Mod. large-scale methanol plants*, pp. 1–12, 2014.

[30] C. Shi, B. Labbaf, E. Mostafavi, and N. Mahinpey, "Methanol production from water electrolysis and tri-reforming: Process design and technical-economic analysis," *J. CO2 Util.*, vol. 38, pp. 241–251, May 2020.

[31] F. Dalena, A. Senatore, A. Marino, A. Gordano, M. Basile, and A. Basile, "Methanol Production and Applications: An Overview," in *Methanol: Science and Engineering*, Elsevier, 2018, pp. 3–28.

[32] K. M. Vanden Bussche and G. F. Froment, "A Steady-State Kinetic Model for Methanol Synthesis and the Water Gas Shift Reaction on a Commercial Cu/ZnO/Al2O3Catalyst," *J. Catal.*, vol. 161, no. 1, pp. 1–10, 1996.

[33] Uniongas, "Chemical Composition of Natural Gas - Union Gas," 2017. [Online]. Available: https://www.uniongas.com/about-us/about-natural-gas/chemical-composition-of-natural-gas. [Accessed: 25-Mar-2019].

[34] K. Li, W. Leigh, P. Feron, H. Yu, and M. Tade, "Systematic study of aqueous monoethanolamine (MEA)-based CO2 capture process: Techno-economic assessment of the MEA process and its improvements," *Appl. Energy*, vol. 165, pp. 648–659, 2016.

[35] Thyssenkrupp, "Hydrogen from large-scale electrolysis," 2018.

[36] "World Energy Outlook 2014," 2014.

[37] É. S. Van-Dal and C. Bouallou, "Design and simulation of a methanol production plant from CO2hydrogenation," *J. Clean. Prod.*, vol. 57, pp. 38–45, 2013.

[38] D. Bellotti, M. Rivarolo, L. Magistri, and A. F. Massardo, "Feasibility study of methanol production plant from hydrogen and captured carbon dioxide," *J. CO2 Util.*, vol. 21, no. July, pp. 132–138, 2017.

[39] M. Pérez-fortes, J. C. Schöneberger, A. Boulamanti, and E. Tzimas, "Methanol synthesis using captured CO 2 as raw material : Techno-economic and environmental assessment," *Appl. Energy*, vol. 161, pp. 718–732, 2016.

[40] W.-H. Cheng, H. H. Kung, and M. Dekker, *Methanol Production and Use*. New York, 1994.

[41] K. C. Shulenberger, A.M., Jonsson, F.R., Ingolfsson, O., Tran, "Process for producing liquid fuel from carbon dioxide and water," 2011.

[42] "MefCO2 (Methanol fuel from CO2) - Synthesis of methanol from captured carbon dioxide using surplus electricity. | SPIRE." [Online]. Available: https://www.spire2030.eu/mefco2. [Accessed: 24-Jun-2019].

[43] "FReSMe (From Residual Steel Gases to Methanol)." [Online]. Available: http://www.fresme.eu/. [Accessed: 24-Jun-2019].

[44] T. Haganuma and D. Fujita, "(12) Patent Application Publication (10) Pub. No.: US 2013/0237618 A1," vol. 1, no. 19, 2013.

[45] K. Li, J. Liu, X. Li, H. Lian, and X. Zhu, "Novel power-to-syngas concept for plasma catalytic reforming coupled with water electrolysis," *Chem. Eng. J.*, vol. 353, no. July, pp. 297–304, 2018.

[46] M. Carmo, D. Fritz, J. Mergel, and D. Stolten, "A Comprehensive review on PEM water electrolysis. Int J Hydrogen Energy ;38:4901-34.," vol. 8, no. 1, 2013.

[47] R. L. Leroy, "I n d u s t r i a l w a t e r electrolysis: present a n d f u t u r e," vol. 8, no. 6, pp. 401–417, 1983.

[48] N. Guillet and P. Millet, "4 Alkaline Water Electrolysis," pp. 117–166, 2018.

[49] K. Zeng and D. Zhang, "Recent progress in alkaline water electrolysis for hydrogen production and applications," *Prog. Energy Combust. Sci.*, vol. 36, no. 3, pp. 307–326, 2010.

[50] C. Song and W. Pan, "Tri-reforming of methane: A novel concept for catalytic production of industrially useful synthesis gas with desired H2/CO ratios," *Catal. Today*, pp. 463–484, 2004.

[51] W. Cho *et al.*, "Optimal design and operation of a natural gas tri-reforming reactor for DME synthesis," *Catal. Today*, 2009.

[52] S. Arora and R. Prasad, "RSC Advances An overview on dry reforming of methane : strategies to reduce carbonaceous deactivation of," pp. 108668–108688, 2016.

[53] Aspen Technology Inc., "Aspen HYSYS Version 10.0," 2017. [Online]. Available: https://www.aspentech.com. [Accessed: 26-Mar-2019].

[54] J. R. Couper, W. R. Penney, J. R. Fair, and S. M. Walas, *Chemical process equipment selection and design*. Gulf Professional Publishing, 2012.

[55] Po-Chuang C., Hsiu-Mei C., Yau-Pin C., Chiou-Shia Y., "Process simulation study of coal to methanol based on gasification technology.," *World Acad. ofScience, Eng. Technol.*, vol. 41, no. 5, pp. 988–996, 2010.

[56] "IPCC, 2014: Climate Change 2014: Synthesis Report. Contribution of Working Groups I, II and III to the Fifth Assessment Report of the Intergovernmental Panel on Climate Change [Core Writing Team, R.K. Pachauri and L.A. Meyer (eds.)]. IPCC, Geneva, Switzer."

[57] J. Kim *et al.*, "Methanol production from CO 2 using solar-thermal energy: Process development and techno-economic analysis," *Energy Environ. Sci.*, vol. 4, no. 9, pp. 3122–3132, 2011.

[58] "Net Generation by Energy Source: Total (All Sectors)," *U.S. Energy Information Administration*, 2019. [Online]. Available: https://www.eia.gov/electricity/monthly/epm_table_grapher.php?t=epmt_1_01.

[Accessed: 13-Jun-2019].

[59] U.S. BUREAU OF LABOR STATISTICS, “United States Core Inflation Rate | 2019 | Data | Chart | Calendar.” [Online]. Available: https://tradingeconomics.com/united-states/core-inflation-rate. [Accessed: 03-Jun-2019].

[60] M. S. Peters and K. D. Timmerhaus, *Plant Design and Economics for Chemical Engineers*. Mcgraw-Hill College Division, 1990.

[61] G. D. Ulrich and P. T. Vasudevan, *Chemical Engineering: Process Design and Economics A Practical Guide*, 2nd ed. Durham, NH: Process Publishing, 2004.

[62] K. Pomerleau, “US Corporate Income Tax Now More Competitive | Tax Foundation,” 2018. [Online]. Available: https://taxfoundation.org/us-corporate-income-tax-more-competitive/. [Accessed: 04-Jun-2019].

[63] Scott Jenkins, “Chemical Engineering Plant Cost Index: 2018 Annual Value - Chemical Engineering | Page 1,” 2019. [Online]. Available: https://www.chemengonline.com/2019-cepci-updates-january-prelim-and-december-2018-final/. [Accessed: 06-Jun-2019].

[64] “Technology Handbook - Air Liquide Engineering & Construction,” 2018.

[65] Nexant Inc., “Equipment Design and Cost Estimation for Small Modular Biomass Systems , Synthesis Gas Cleanup , and Oxygen Separation Equipment,” *NREL Rep. SR-510-39945*, no. May, pp. 1–117, 2006.

[66] BUREAU OF LABOR STATISTICS, “Occupational Employment and Wages, May 2018 51-8091 Chemical Plant and System Operators,” 2019. [Online]. Available: https://www.bls.gov/oes/current/oes518091.htm. [Accessed: 07-Jun-2019].

[67] “Henry Hub Natural Gas Spot Price (Dollars per Million Btu),” 2018. [Online]. Available: https://www.eia.gov/dnav/ng/hist/rngwhhdm.htm. [Accessed: 26-Mar-2019].

[68] “Industrial Price Comparison,” 2018. [Online]. Available: https://www.rockymountainpower.net/about/rar/ipc.html. [Accessed: 26-Mar-2019].

[69] “Pricing | Methanex Corporation,” 2019. [Online]. Available: https://www.methanex.com/our-business/pricing. [Accessed: 22-Mar-2019].

[70] H. Herzog and K. Smekens, “IPCC Special Report on Carbon Dioxide Capture and Storage,” 2018.

Appendix A**: Re-arrangement of Kinetics Expression for Aspen HYSYS**

Original Kinetics:

The governing equations and kinetic rate expressions for methanol synthesis are retrieved from Vanden Bussche and G.F. Froment:

CO_2 hydrogenation: $CO_2 + 3H_2 \rightarrow CH_3OH + H_2O, \quad \Delta H^o = -49 \text{ kJ mol}^{-1}$

WGS: $CO + H_2O \leftrightarrow CO_2 + H_2, \quad \Delta H^o = -41 \text{ kJ mol}^{-1}$

<table>
<tr><td colspan="2">Methanol Synthesis:
$r_{CH3OH} = \frac{k_1 P_{CO2} P_{H2}\left(1-\frac{1}{K_{eq1}}\frac{P_{H2O}P_{CH3OH}}{P_{H2}^3 P_{CO2}}\right)}{\left(1+k_2\frac{P_{H2O}}{P_{H2}}+k_3 P_{H2}^{0.5}+k_4 P_{H2O}\right)^3}$</td><td colspan="2">WGS:
$r_{WGS} = \frac{k_5 P_{CO2}\left(1-K_{eq2}\frac{P_{H2O}P_{CO}}{P_{CO2}P_{H2}}\right)}{\left(1+k_2\frac{P_{H2O}}{P_{H2}}+k_3 P_{H2}^{0.5}+k_4 P_{H2O}\right)}$</td><td rowspan="2">$r\left[\frac{mol}{kg_{cat}\cdot s}\right]$</td></tr>
<tr><td colspan="2">$\log_{10}K_{eq1} = \frac{3066}{T} - 10.592$</td><td colspan="2">$\log_{10}\frac{1}{K_{eq2}} = -\frac{2073}{T} + 2.029$</td></tr>
<tr><td>$k_1 = 1.07\exp\left(\frac{36696}{RT}\right)$</td><td>$k_2 = 3453.38$</td><td>$k_3 = 0.499\left(\frac{17197}{RT}\right)$</td><td rowspan="2">T [K]

P[bar]</td></tr>
<tr><td colspan="2">$k_4 = 6.62E-11\left(\frac{124119}{RT}\right)$</td><td colspan="2">$k_5 = 1.22E10\exp\left(\frac{-94765}{RT}\right)$</td></tr>
</table>

Table A1 Kinetic expressions

In order to model this LHHW expression in Aspen HYSYS, the kinetic data must be re-arranged in the following manner:

rate=Numerator/Denominator

Numerator=k*f(Basis) - k'*f'(Basis)

Denominator=(1 + K1*f1(Basis) + K2*f2(Basis) + ...)^n

k = A * exp { -E / RT } * T ^ß k' = A' * exp { -E' / RT } * T^ß'

K1 = A1 * exp{-E1/RT}, K2 = A2 * exp{-E2/RT}, ...

The functions of the Basis (f, f', f1, f2, ...) are the product of 'concentrations' (in the Basis units) to the power of the specified exponents.

The indexes 1, 2, ... in the constants K, A, and E indicate the row number in the matrix of denominator terms.

n is the denominator exponent

Re-arrangements:

Equilibrium Constants (K_{eq1}, K_{eq2}):

$$\log_{10}K_{eq1} = \frac{3066}{T} - 10.592 \qquad \log_{10}\frac{1}{K_{eq2}} = -\frac{2073}{T} + 2.029$$

$$K_{eq1} = 10^{\frac{3066}{T}-10.592} \qquad K_{eq2} = 10^{\frac{2073}{T}-2.029}$$

$$\ln(K_{eq1}) = \ln(10^{\frac{3066}{T}-10.592}) \qquad \ln(K_{eq2}) = \ln(10^{\frac{2073}{T}-2.029})$$

$$\ln(K_{eq1}) = \ln(10) * (\frac{3066*8.314}{T*R} - 10.592) \qquad \ln(K_{eq2}) = \ln(10) * (\frac{2073*8.314}{T*R} - 2.029)$$

$$K_{eq1} = e^{(\frac{\ln(10)*3066*8.314}{T*R}-\ln(10)*10.592)} \qquad K_{eq2} = e^{(\frac{\ln(10)*2073*8.314}{T*R}-\ln(10)*2.029)}$$

$$K_{eq1} = e^{(\frac{58695}{T*R}-24.39)} \qquad K_{eq2} = e^{(\frac{39685}{T*R}-4.67)}$$

$$K_{eq1} = 2.56E-11exp^{(\frac{58695}{RT})} \qquad K_{eq2} = 9.35E-3exp^{(\frac{39685}{RT})}$$

CO_2 hydrogenation:

$$r_{CH3OH} = \frac{k_1 P_{CO2} P_{H2} \left(1 - \frac{1}{K_{eq1}} \frac{P_{H2O} P_{CH3OH}}{P_{H2}^3 P_{CO2}}\right)}{\left(1 + k_2 \frac{P_{H2O}}{P_{H2}} + k_3 P_{H2}^{0.5} + k_4 P_{H2O}\right)^3}$$

$$r_{CH3OH} = \frac{k_1 P_{CO2} P_{H2} - \frac{k_1}{K_{eq1}} \frac{P_{H2O} P_{CH3OH}}{P_{H2}^2}}{\left(1 + k_2 \frac{P_{H2O}}{P_{H2}} + k_3 P_{H2}^{0.5} + k_4 P_{H2O}\right)^3}$$

$$r_{CH3OH} = \frac{1.07\exp\left(\frac{36696}{RT}\right) P_{CO2} P_{H2} - \frac{1.07\exp\left(\frac{36696}{RT}\right)}{2.56E-11 exp^{\left(\frac{58695}{RT}\right)}} \frac{P_{H2O} P_{CH3OH}}{P_{H2}^2}}{\left(1 + 3453.38 \frac{P_{H2O}}{P_{H2}} + 0.499 \left(\frac{17197}{RT}\right) P_{H2}^{0.5} + 6.62E-11 \left(\frac{124119}{RT}\right) P_{H2O}\right)^3}$$

$$r_{CH3OH} = \frac{1.07\exp\left(\frac{36696}{RT}\right) P_{CO2} P_{H2} - 4.18E10\exp\left(\frac{-21999}{RT}\right) \frac{P_{H2O} P_{CH3OH}}{P_{H2}^2}}{\left(1 + 3453.38 \frac{P_{H2O}}{P_{H2}} + 0.499 \left(\frac{17197}{RT}\right) P_{H2}^{0.5} + 6.62E-11 \left(\frac{124119}{RT}\right) P_{H2O}\right)^3}$$

The reaction rate by default from literature is expressed in $\frac{mol}{kg_{cat} \cdot s}$. In HYSYS, the reaction rate is commonly expressed in $\frac{kgmole}{m^3 s}$. Therefore further unit conversions are necessary:

$$r_{CH3OH} = \frac{1.07\exp\left(\frac{36696}{RT}\right) P_{CO2} P_{H2} - 4.18E10\exp\left(\frac{-21999}{RT}\right) \frac{P_{H2O} P_{CH3OH}}{P_{H2}^2}}{\left(1 + 3453.38 \frac{P_{H2O}}{P_{H2}} + 0.499 \left(\frac{17197}{RT}\right) P_{H2}^{0.5} + 6.62E-11 \left(\frac{124119}{RT}\right) P_{H2O}\right)^3} * \frac{1140 kg_{cat}}{m^3} * \frac{1 \text{ kgmole}}{1000 \text{ mole}}$$

$$r_{CH3OH} = \frac{1.22\exp\left(\frac{36696}{RT}\right) P_{CO2} P_{H2} - 4.77E10\exp\left(\frac{-21999}{RT}\right) \frac{P_{H2O} P_{CH3OH}}{P_{H2}^2}}{\left(1 + 3453.38 \frac{P_{H2O}}{P_{H2}} + 0.499 \left(\frac{17197}{RT}\right) P_{H2}^{0.5} + 6.62E-11 \left(\frac{124119}{RT}\right) P_{H2O}\right)^3}$$

Water Gas Shift (WGS):

$$r_{WGS} = \frac{k_5 P_{CO2}\left(1 - K_{eq2}\frac{P_{H2O}P_{CO}}{P_{CO2}P_{H2}}\right)}{\left(1 + k_2\frac{P_{H2O}}{P_{H2}} + k_3 P_{H2}^{0.5} + k_4 P_{H2O}\right)}$$

$$r_{WGS} = \frac{k_5 P_{CO2} - k_5 K_{eq2}\frac{P_{H2O}P_{CO}}{P_{H2}}}{\left(1 + k_2\frac{P_{H2O}}{P_{H2}} + k_3 P_{H2}^{0.5} + k_4 P_{H2O}\right)}$$

$$r_{WGS} = \frac{1.22E10\exp\left(\frac{-94765}{RT}\right)P_{CO2} - 1.22E10\exp\left(\frac{-94765}{RT}\right) * 9.35E-3exp^{\left(\frac{39685}{RT}\right)} * \frac{P_{H2O}P_{CO}}{P_{H2}}}{\left(1 + k_2\frac{P_{H2O}}{P_{H2}} + k_3 P_{H2}^{0.5} + k_4 P_{H2O}\right)}$$

$$r_{WGS} = \frac{1.22E10\exp\left(\frac{-94765}{RT}\right)P_{CO2} - 1.14E8\exp\left(\frac{-55080}{RT}\right) * \frac{P_{H2O}P_{CO}}{P_{H2}}}{\left(1 + k_2\frac{P_{H2O}}{P_{H2}} + k_3 P_{H2}^{0.5} + k_4 P_{H2O}\right)}$$

$$r_{WGS} = \frac{1.22E10\exp\left(\frac{-94765}{RT}\right)P_{CO2} - 1.14E8\exp\left(\frac{-55080}{RT}\right) * \frac{P_{H2O}P_{CO}}{P_{H2}}}{\left(1 + k_2\frac{P_{H2O}}{P_{H2}} + k_3 P_{H2}^{0.5} + k_4 P_{H2O}\right)} * \frac{1140 kg_{cat}}{m^3} * \frac{1\ kgmole}{1000\ mole}$$

$$r_{WGS} = \frac{1.39E10\exp\left(\frac{-94765}{RT}\right)P_{CO2} - 1.30E8\exp\left(\frac{-55080}{RT}\right) * \frac{P_{H2O}P_{CO}}{P_{H2}}}{\left(1 + k_2\frac{P_{H2O}}{P_{H2}} + k_3 P_{H2}^{0.5} + k_4 P_{H2O}\right)}$$

Lastly, the kinetic parameters in the highlighted equations are used for HYSYS reactor modeling.

Appendix B**: Capital Cost Estimation**

Calculation steps:

1. Compile a list of equipment from process simulation
2. Equipment sizing and purchase cost estimation
3. Factor in offsite costs, contingency and working capital

List of equipment:

Water Electrolysis	Alkaline Water Electrolysis Plant
Tri-reforming	Tri-Reformer Feed Gas Pre-Heater Pre-Reformer Waste Heat Boiler ATR Effluent Cooler Pre-heater Air Blower
Compression	Syngas Compressor Stage 1 Syngas Compressor Stage 2 Recycled Gas Compressor Syngas Compressor Stage 1 Turbine Syngas Compressor Stage 2 Turbine Recycled Gas Compressor Turbine Syngas Compressor Inter-stage Cooler Syngas Compressor Suction Scrubber
Methanol Synthesis	Methanol Reactor Methanol Reactor Feed/Effluent Exchanger
Purification	Methanol/Water Distillation Tower Recycle Gas Flash Drum Purge Gas Flash Drum Reactor Effluent/Column feed exchanger Reactor Effluent Cooler Methanol/Water Tower Condenser Methanol/Water Tower Reboiler
Utilities	Boiler Feed Water Surge Vessel BFW Pump Make-up Water Pump Cooling Water Circulation Pump Make-up Water Preheater

Equipment Sizing and Cost Estimation:

Water Electrolysis System: Alkaline Water Electrolyser	Cost for the water electrolysis system is taken directly from tKUCE: $375 million ±35% Off-site facilities such as water treatment, utilities and gas compression are assumed to be 30% of the total cost. They are subtracted from the total cost in order to get an estimate on the bare module cost. 375 – 0.30*375 = 262 Bare module cost = $262,500,000
Tri-Reforming System: Tri-reformer Feed Gas Pre-Heater Pre-Reformer Waste Heat Boiler ATR Effluent Cooler Pre-heater Air Blower	To account for economy of scale, the following formula is used in the cost estimation of the tri-reforming system: New cost = Base cost * (New capacity/Base capacity)^n Cost data from Air Liquide are used: 500,000 Nm3/h of syngas (160 mil) 1,000,000 Nm3/h of syngas (280 mil) n = 0.637 The tri-reforming system in the process has a net syngas production of 207,000 Nm3/h Bare module cost = $92,000,000
Syngas Compressor Stage 1	- Purchase price at $5.0 mil for 7936 kW (U&V Figure 5.30) - cost index for 2018 is 603.1, U&V reference is 400 - Bare module factor for centrifugal carbon steel compressor is 2.5 Bare module cost = $18,843,750
Syngas Compressor Stage 2	- Purchase price at $5.5 mil for 8971kW (extrapolated from U&V Fig 5.30) - cost index for 2018 is 603.1, U&V reference is 400 - Bare module factor for centrifugal carbon steel compressor is 2.5 Bare module cost = $20,728,125
Recycled Gas Compressor	- Purchase price at $1.75 mil for 2363 kW (extrapolated from U&V Fig 5.30) - cost index for 2018 is 603.1, U&V reference is 400 - Bare module factor for centrifugal carbon steel compressor is 2.5 Bare module cost = $6,595,313
Syngas Compressor Stage 1 Turbine	- Purchase price at $450,000 for 7936 kW (extrapolated from U&V Fig 5.20) - cost index for 2018 is 603.1, U&V reference is 400 - Bare module factor for centrifugal carbon steel compressor turbine is 1.5 Bare module cost = $1,017,563
Syngas Compressor	- Purchase price at $500,000 for 8971 kW (extrapolated from

Stage 2 Turbine	U&V Fig 5.20) - cost index for 2018 is 603.1, U&V reference is 400 - Bare module factor for centrifugal carbon steel compressor turbine is 1.5 Bare module cost = $1,130,625
Recycled Gas Compressor Turbine	- Purchase price at $500,000 for 2363 kW (extrapolated from U&V Fig 5.20) - cost index for 2018 is 603.1, U&V reference is 400 - Bare module factor for centrifugal carbon steel compressor turbine is 1.5 Bare module cost = $339,188
Syngas Compressor Inter-stage Cooler	U = 1206W/m2K (from U&V Table 4-15a) Overall UA [kJ/C-h] = 4.811E5 (from HYSYS) Total heat transfer area = 111 m2 From U&V Figure 5.44: Take fixed tube sheet HEX at 111 m2 with purchase cost at $13,000 This process requires 1 HEX Total purchase cost is $13,000 - cost index for 2018 is 603.1, U&V reference is 400 Pressure factor = 1.25 Bare Module factor = 3 Bare module cost = $58,793
Syngas Compressor Suction Scrubber	Vessel Size (From HYSYS sizing calc.): L: 8.0m x D: 2.3m V: 33m^3 From U&V Figure 5.44: Equipment purchase cost = $13,000 - cost index for 2018 is 603.1, U&V reference is 400 Pressure factor = 2.5 Material factor (Stainless Steel) = 4.0 FBM = 20 Bare module cost = $1,206,000
Methanol Reactor	Assume the reactor internal design is similar to a shell and tube heat exchanger # of tubes = 2700 Tube length = 7 m Tube diameter = 0.035 m Total estimated area is 2078 m2 extrapolate graph on U&V Fig 5.36 Purchase cost of equipment is $100,000 - cost index for 2018 is 603.1, U&V reference is 400 Pressure factor = 1.2 FBM = 3.5 Bare module cost = $527,625
Methanol Reactor Feed/Effluent	U = 1859 W/m2K (from U&V Table 4-15a) Overall UA [kJ/C-h] = 1.03E7 (From HYSYS)

Exchanger	The total heat transfer area is estimated to be 1541 m2 Referenced from U&V 5.36: 2 fixed tube sheet HEX at 800 m2. purchase cost at $40000 per HEX Total purchase cost is $80000 - cost index for 2018 is 603.1, U&V reference is 400 Pressure factor = 1.15 Bare Module factor = 3.5 Bare module cost = $422,100
Methanol/Water Distillation Tower	Tower cost = Vessel + trays Estimated Height and Diameter (from HYSYS Sizing calc.): 29 m x 5.3 m From U&V Figure 5.44 Vessel Purchase cost: $250,000 Tray purchase cost: 35 * $1,200 - cost index for 2018 is 603.1, U&V reference is 400 Pressure factor = 1.2 Material factor (Stainless Steel) = 4.0 Bare module factor = 11 Bare module cost = $4,842,090
Recycle Gas Flash Drum	Vessel Size (From HYSYS sizing calc.): L: 13.3 m x D: 3.8 m V: 152 m^3 From U&V Figure 5.44: Equipment purchase cost = $90,000 - cost index for 2018 is 603.1, U&V reference is 400 Pressure factor (1.02E4 kPa) = 5.5 Material Factor (Stainless Steel) = 4.0 Bare Module factor = 40 Bare module cost = $5,427,000
Purge Gas Flash Drum	Vessel Size (From HYSYS sizing calc.): L: 8.4 m x D: 1.5 m V: 15.3 m^3 From U&V Figure 5.44: Equipment purchase cost = $25,000 - cost index for 2018 is 603.1, U&V reference is 400 Pressure factor (250 kPa) = 1.2 Material Factor (Stainless Steel) = 4.0 Bare Module factor = 11 Bare module cost = $414,563
Reactor Effluent/Column feed exchanger	U = 200 W/m2K (from U&V Table 4-15a) Overall UA [kJ/C-h] = 3.06E6 (From HYSYS) The total heat transfer area is estimated to be 4260 m2 Referenced from U&V Figure 5.36: Total purchase cost is $250,000 (5 HEX) - cost index for 2018 is 603.1, U&V reference is 400 Pressure factor (1.04E4 kPa) = 1.15 Material factor (Stainless Steel) = 3.00

	Bare Module factor = 6.5 Bare module cost = $2,449,688
Reactor Effluent Cooler	U = 200 W/m2K (from U&V Table 4-15a) Overall UA [kJ/C-h] = 6.95E6 (From HYSYS) Estimated heat transfer area = 8241m2 Referenced from U&V Figure 5.36: Max area for fixed tube sheet HEX is 900 m2 with purchase cost at $55000 Total purchase cost is $440,000 (8 HEX) - cost index for 2018 is 603.1, U&V reference is 400 Pressure factor (1.04E4 kPa) = 1.15 Material factor (Stainless Steel) = 3 Bare Module factor = 6 Bare module cost = $3,979,800
Distillation Tower Condenser	U = 950 W/m2K (from U&V Table 4-15a) Assume LMTD = 20 Overall duty [kJ/C-h] = 2.42E8 (From HYSYS) Estimated heat transfer area is 3538 m2 Referenced from U&V 5.36: Using graph extrapolation: purchase cost is at ~$180,000 - cost index for 2018 is 603.1, U&V reference is 400 Pressure factor = 1.15 Material factor (CS/SS) = 1.7 Bare Module factor = 4.5 Bare module cost = $1,221,075
Distillation Tower Reboiler	U = 1400 W/m2K (from U&V Table 4-15a) Assume LMTD = 110 Overall duty [kJ/C-h] = 2.43E8 (From HYSYS) Estimated heat transfer area is 438 m2 Referenced from U&V 5.36: Extrapolate graph with purchase cost at $25,000 - cost index for 2018 is 603.1, U&V reference is 400 Pressure factor = 1.15 Material factor (SS) = 3 Bare Module factor = 6 Bare module cost = $316,575
Boiler Feed Water Surge Vessel	Vessel Size (From HYSYS sizing calc.): L: 6.5 m x D: 2.5 m V: 32 m^3 From U&V Figure 5.44: Equipment purchase cost = $33,000 - cost index for 2018 is 603.1, U&V reference is 400 Pressure factor (4250 kPa) = 3.5 Material Factor (Stainless Steel) = 4.0 Bare Module factor = 8.5 Bare module cost = $422,854

BFW Pump	- Purchase price at $12000 for 22 kW (U&V Figure 5.49) - cost index for 2018 is 603.1, U&V reference is 400 Pressure factor (2300 kPa) = 2.5 Material factor (SS) = 1.9 Bare module factor = 9 Bare module cost = $162,810
Make-up Water Pump	- Purchase price at $15000 for 28 kW (U&V Figure 5.49) - cost index for 2018 is 603.1, U&V reference is 400 Pressure factor (2300 kPa) = 2.5 Material factor (SS) = 1.9 Bare module factor = 9 Bare module cost = $162,810
Cooling Water Circulation Pump	- Purchase price at $40000 for 295 kW (U&V Figure 5.49) - cost index for 2018 is 603.1, U&V reference is 400 Pressure factor (400 kPa) = 1 Material factor (SS) = 1.9 Bare module factor = 5 Bare module cost = $301,500
Make-up Water Preheater	U = 1300 W/m2K (from U&V Table 4-15a) Assume LMTD = 112C Overall duty [kJ/C-h] = 1.78E7 (From HYSYS) Estimated heat transfer area is 34 m2 Referenced from U&V 5.36: purchase cost is at ~$600 - cost index for 2018 is 603.1, U&V reference is 400 Pressure factor = 1.15 Material factor (SS) = 3.0 Bare Module factor = 6 Bare module cost = $54,270

Cost Summary:

Water Electrolysis	$262,500,000
Tri-reforming	$92,000,000
Syngas Compressor Stage 1	$18,843,750
Syngas Compressor Stage 2	$20,728,125
Recycled Gas Compressor	$6,595,313
Syngas Compressor Stage 1 Turbine	$1,017,563
Syngas Compressor Stage 2 Turbine	$1,130,625
Recycled Gas Compressor Turbine	$339,188
Syngas Compressor Inter-stage Cooler	$58,793
Syngas Compressor Suction Scrubber	$1,206,000
Methanol Reactor	$527,625
Methanol Reactor Feed/Effluent Exchanger	$422,100
Methanol/Water Distillation Tower	$4,842,090
Recycle Gas Flash Drum	$5,427,000
Purge Gas Flash Drum	$414,563
Reactor Effluent/Column feed exchanger	$2,449,688
Reactor Effluent Cooler	$3,979,800
Methanol/Water Tower Condenser	$1,221,075
Methanol/Water Tower Reboiler	$316,575
Boiler Feed Water Surge Vessel	$422,854
BFW Pump	$162,810
Make-up Water Pump	$203,513
Cooling Water Circulation Pump	$301,500
Make-up Water Preheater	$54,270
Total	**$420,535,406**

Other Cost Factors:

- Offsite facilities: 30% of plant bare module. This includes any auxiliary buildings, product storage tanks, chemical supplies and miscellaneous utilities.
  Offsite cost = 0.30 * $420,535,406 = $126,160,622
- Project contingency: 30% of plant bare module. This accounts for unforeseen expenses, unexpected delays, disruptive weather etc.

  Contingency cost = 0.30 * $420,535,406 = $126,160,622
- Fixed capital is the summation of plant bare module, offsite and contingency costs

  Fixed capital = $420,535,406 + $126,160,622 + $126,160,622 = $672,856,649
- Working capital: 15% of fixed capital. The fixed capital cost is the summation of plant bare module, offsite facilities and project contingency.

  Working capital = 0.15 * $672,856,649 = $100,928,497
- Total capital cost is the summation of fixed capital and working capital.

  CAPEX = $672,856,649 + $100,928,497 = $773,785,147 = $ 774 million

Appendix C**: Operating Cost Estimation**

Calculation steps:

Operating cost is divided into direct and indirect expenses.

Direct expenses include: Raw materials (natural gas, demineralized water, carbon dioxide), catalysts (Ni/Al2O3, Cu/ZnO), operating labor, supervision, utilities (Electricity, steam, cooling water), maintenance and repairs, operating supplies, laboratory charges, patents and royalties.

Indirect expenses include: Overhead, local taxes, insurance

Base assumptions and method of calculation for each expense item:

Location	US Texas
Time	2018
Currency	US Dollar
On Stream Factor	0.91
Direct expenses:	
Natural gas	Annual Consumption (from HYSYS): 3.05E8 kg/year Natural gas composition is obtained from Union Gas Price is retrieved from Henry Hub Data 2018 3.17 $/MMBtu (3.00$/GJ) HYSYS LHV of Natural Gas: 48320 KJ/kg (0.048320 GJ/kg) Unit Price: 3*0.048320 = 0.145$/kg
Demineralized water	Annual Consumption (from HYSYS): 3.59E5 m3/year Reference according to U&V Equation 6.1: Csu = a * CEI + b * Csf For demineralized water grassroot: a = 0.007+2.5e-4*q^-0.6 b = 0.004 CEI = 567 Csf = 3.10 $/GJ q = 45.09 m3/h = 0.013 m3/s Unit price = Csu = 5.95$/m3
Carbon dioxide	Annual Consumption (from HYSYS): 2.36E8 kg/year

	$86.40/t - The current price of CO2 capture from a coal combustion plant using amine absorption technology (Li et al. 2016)
Ni/Al2O3 Catalyst	GHSV = reactant std, volumetric flow/catalyst volume Pre-reformer Reactor Assume GHSV = 3000 h-1 std volumetric flow = 77140 m3/h Catalyst volume = 26m3 TRM reactor Assume GHSV = 3000 h-1 Std volumetric flow = 200700 m3/h Catalyst volume = 67m3 total catalyst volume = ~93 m3 Assume catalyst density = 2000 kg/m3 Void fraction = 0.4 Total catalyst loading: 111.6 Mt Assume 5 year replacement Annual catalyst assumption: 22.3 Mt/year Catalyst price taken from NREL (2011): $21.36/kg 2011 CEI = 585.7 2018 CEI = 567 Catalyst price for 2018: $20.6/kg
Cu/ZnO Catalyst	Bulk Density: 1140 kg/m3 Total reactor tube side volume: 18.18 m3 Total catalyst loading is 20.7 Mt Assume catalyst lifetime = 5 yrs Annual catalyst consumption:4 Mt/year Catalyst price taken from NREL (2011): $21.36/kg 2011 CEI = 585.7 2018 CEI = 567 Catalyst price for 2018: $20.6/kg
Operating labor	Total number of operators per shift: Water Electrolysis = 4 ATR = 2 Compression = 1 Methanol reactor = 1 Purification = 1 Utilities = 1

	Total = 10 Assume 3 shifts per day According to the US Bureau of Labor Statistics, annual salary per worker is $62380
Supervision	10% of operating labor
Electricity	Annual Consumption (from HYSYS): 2.56E9 kWh/year Rocky Mountain Power electricity rates of 2018: 5.57 cents/kWh
Steam	Annual Consumption (from HYSYS): 0 kg/year Reference U&V Equation 6.1: Csu = a * CEI + b * Csf For Process Steam Grassroot: a = 2.3 * ms^(-0.9) b = 0.0034*P^(0.05) CEI = 567 ms =24.675 kg/s P = 39.13 bar Csu = 0.013 $/kg
Cooling water	Annual Consumption (from HYSYS): 6.30E7 m3/year Reference U&V Equation 6.1: Csu = a * CEI + b * Csf For cooling water grassroot: a = 0.00007+2.5e-5*q^-1 b = 0.003 CEI = 567 Csf = 3.10 $/GJ q = 2556 m3/h + 6488 m3/h = 9044 m3/h = 2.51 m3/s Csu = 0.054$/m3
Maintenance and repairs	2% of fixed capital
Operating supplies	10% of maintenance
Laboratory charges	10% of operating labor
Patents and royalties	2% of direct expense
Indirect expenses:	
Overhead	50% of operating labour supervision and maintenance
Local taxes	2% of fixed capital
Insurance	1% of fixed capital

Operating cost summary:

Date	2019-11-28	
Job Title	Electrolysis + ATR Methanol Facility	
Location	US/CAN	
Currency	USD	
On Stream Factor	0.91	333 days

Direct	Annual Cost ($/yr)		Unit Price	
1. Raw Materials				
Natural Gas	$	44,266,610.13	145.00	$/Mt
Demineralized Water	$	2,139,858.00	5.95	$/m3
Carbon dioxide (CO2)	$	20,399,848.32	86.40	$/Mt
2. Catalysts				
Ni/Al2O3 (ATR + pre-reformer)	$	446,000.00	20000	$/Mt
Cu/ZnO (MeOH Reactor)	$	80,000.00	20000	$/Mt
3. Operating Labor	$	1,871,400.00	62,380.00	$/yr
4. Supervision	$	187,140.00		
5. Utilities				
Electricity	$	142,341,552.84	0.0557	$/kWh
Steam	$	-	0.013	$/kg
Cooling Water	$	3,411,015.75	0.054	$/m3
6. Maintenance and repairs	$	13,457,132.98		
7. Operating supplies	$	1,345,713.30		
8. Laboratory Charges	$	187,140.00		
9. Patents and royalties	$	4,602,668.23		
Subtotal	**$**	**234,736,079.55**		

Indirect	Annual Cost ($/yr)		Unit Price
1. Overhead	$	7,757,836.49	
2. Local Taxes	$	13,457,132.98	
3. Insurance	$	6,728,566.49	
Subtotal	**$**	**27,943,535.97**	

Total Operating Cost	**$**	**262,679,615.52**

Appendix D**: Discounted Cash Flow Analysis**

Table B1 Assumed parameters for the DCF Analysis

Project Life (years)	20
Inflation	1.9%
Depreciation ($M)	31.0
Income Tax	21%
Annual Sales Revenue ($M/yr)	343.3
Annual Operating Cost ($M/yr)	262.7
Annual Discount Rate	8.0%
Fixed Capital ($M/yr)	672.9
Working Capital ($M/yr)	100.9
Total Investment ($M/yr)	773.8
Construction period (Years)	3
Start-up (C&SU) period (Years)	1

DCF formulas:

1. **Net Income** = (Annual Sales Revenue – Operating Cost) * (1 + Inflation) ^(Year – 1)

   (Net income for the initial 3 years is 0 due to constructions. During the start-up year, net income is halved because it is assumed production will only reach 50% of its designed capacity)
2. **Cash Flow** =

   Fixed Capital + Working Capital (Year -2: 25%, Year -1: 25%, Year 0: 50%)

   Net income (From year 1 to 19)

   Net income + Depreciated Value (Year 20)
3. **Depreciated Value** = Fixed Capital – Depreciation * Year Count

   (Depreciation is calculated by assuming straight line depreciation with 20% salvage value)
4. **Taxable Income** = Net Income – Depreciation
5. **Tax** = Income Tax * Taxable Income
6. **Cash Flow After Tax** = Cash Flow – Tax
7. **Discount Factor** = (1 + Annual Discount Rate) ^(-Year)
8. **Discounted Cash Flow (DCF) =** Cash Flow After Tax * Discount Factor
9. **Cumulative DCF** = Adding DCFs from previous years

Table B2. Discounted Cash Flow Table

Year	Net Income ($M)	Cash Flow ($M)	Depreciated Value ($M)	Taxable Income ($M)	Tax ($M)	Cash Flow After Tax ($M)	Disc. Factor	DCF ($M)	Cum. DCF ($M)
-2	0.0	-193.4	0.0	0.0	0.0	-193.4	N/A	-193	-193
-1	0.0	-193.4	0.0	0.0	0.0	-193.4	N/A	-193	-387
0	0.0	-386.9	773.8	0.0	0.0	-386.9	0.00	-387	-774
1	40.3	40.3	742.8	9.4	2.0	38.3	0.00	36	-738
2	82.1	82.1	711.9	51.2	10.8	71.4	0.00	61	-677
3	83.7	83.7	680.9	52.8	11.1	72.6	0.00	58	-619
4	85.3	85.3	650.0	54.3	11.4	73.9	0.00	54	-565
5	86.9	86.9	619.0	56.0	11.8	75.2	0.00	51	-514
6	88.6	88.6	588.1	57.6	12.1	76.5	0.00	48	-466
7	90.2	90.2	557.1	59.3	12.5	77.8	0.00	45	-420
8	92.0	92.0	526.2	61.0	12.8	79.2	0.00	43	-378
9	93.7	93.7	495.2	62.8	13.2	80.5	0.00	40	-337
10	95.5	95.5	464.3	64.5	13.6	81.9	0.00	38	-299
11	97.3	97.3	433.3	66.4	13.9	83.4	0.00	36	-264
12	99.2	99.2	402.4	68.2	14.3	84.8	0.00	34	-230
13	101.0	101.0	371.4	70.1	14.7	86.3	0.00	32	-198
14	103.0	103.0	340.5	72.0	15.1	87.8	0.00	30	-168
15	104.9	104.9	309.5	74.0	15.5	89.4	0.00	28	-140
16	106.9	106.9	278.6	76.0	16.0	91.0	0.00	27	-114
17	108.9	108.9	247.6	78.0	16.4	92.6	0.00	25	-89
18	111.0	111.0	216.7	80.1	16.8	94.2	0.00	24	-65
19	113.1	113.1	185.7	82.2	17.3	95.9	0.00	22	-43
20	115.3	115.3	154.8	84.3	17.7	252.3	0.00	54	11